# SS 433 seen in the Gamma rays

**Jian Li**

**University of Science and Technology of China**

VGGRS VII, 6-8 May 2025, Barcelona

# Black hole (BH) is the most populated gamma-ray sources

(more than half of detected gamma-ray sources)

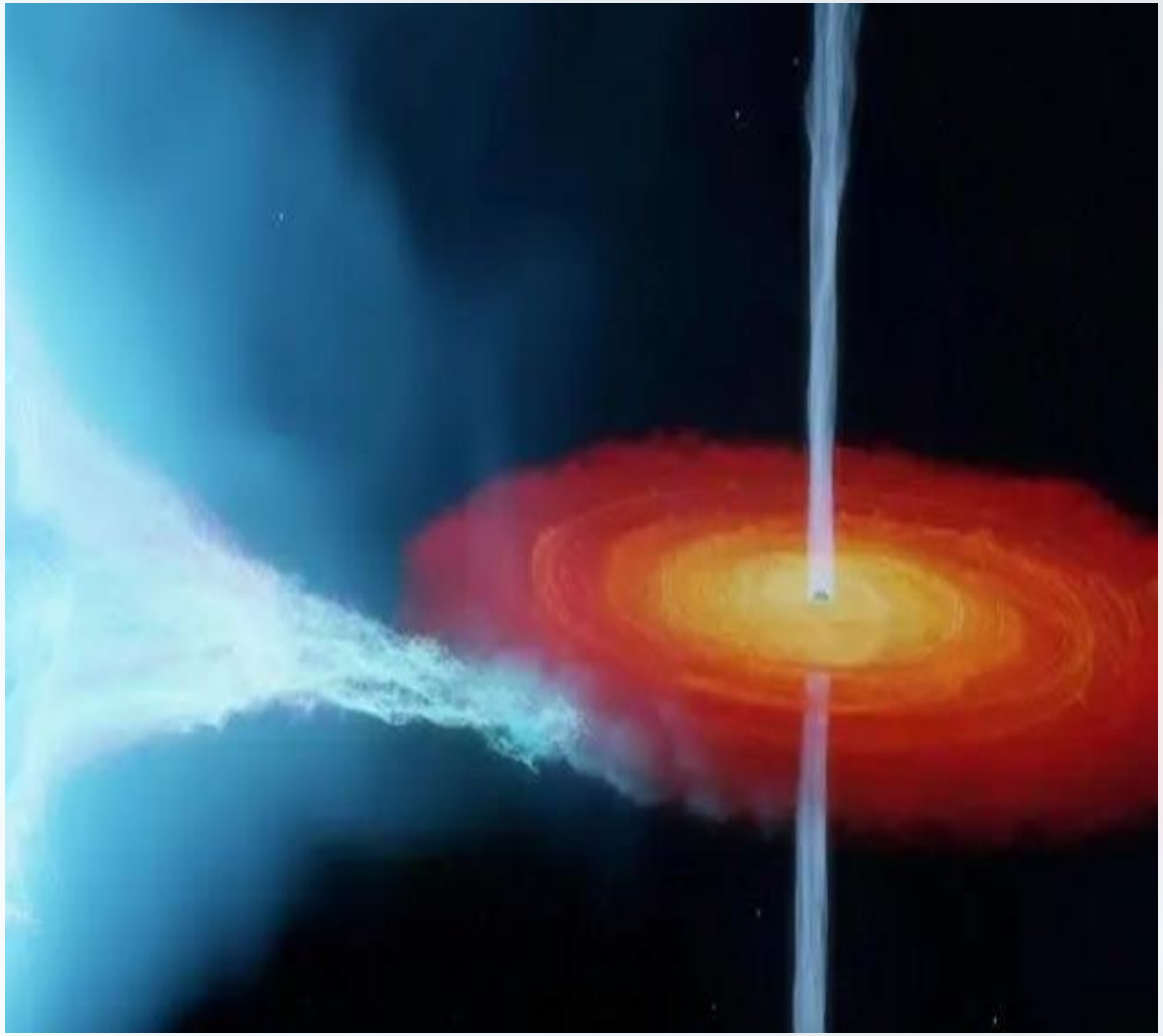

stellar mass BH
(e.g. microquasar)

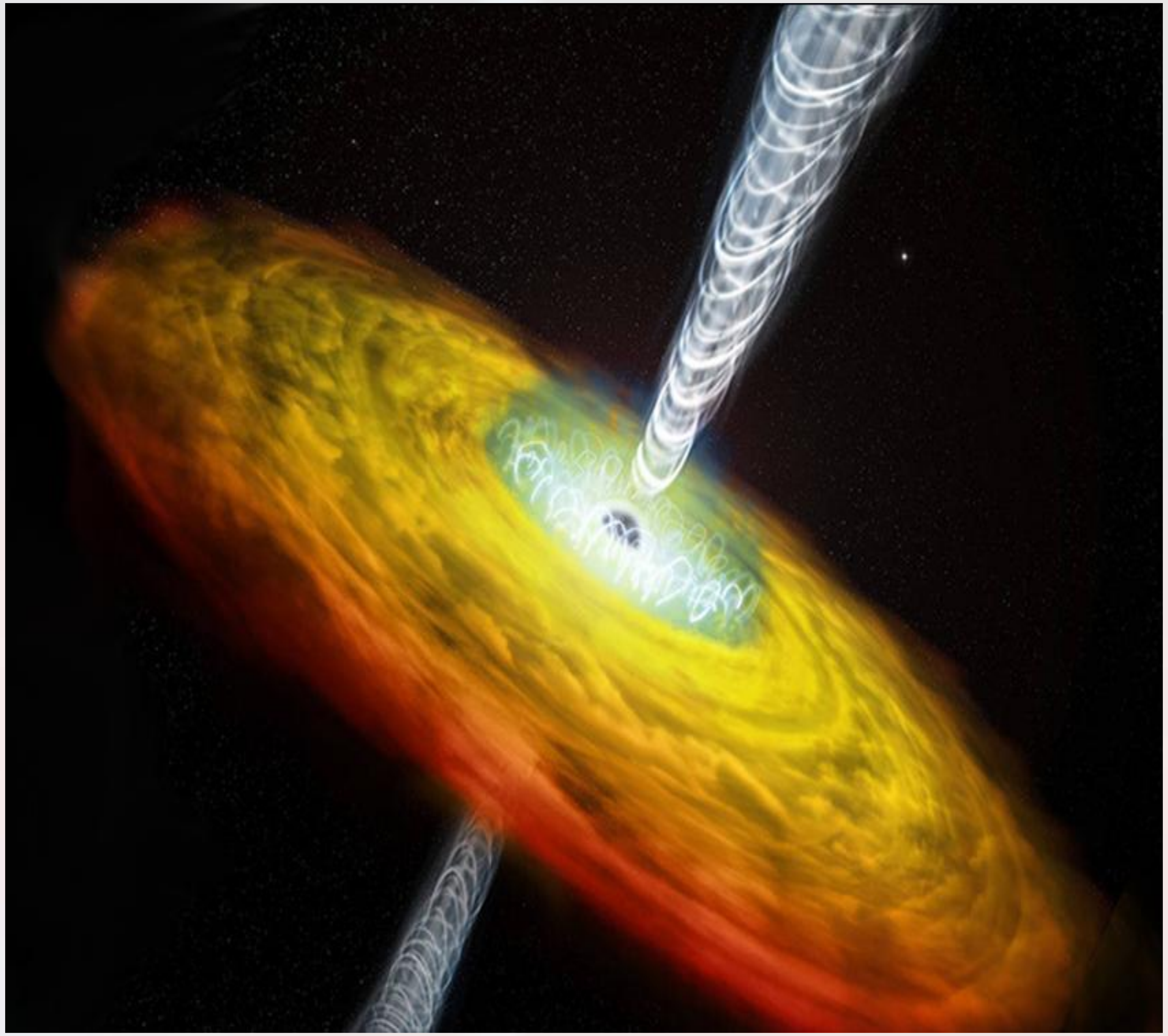

supermassive BH
(e.g. AGNs, blazars)

Where could particle acceleration happen

in a Black Hole system

(stellar mass BH or supermassive BH)?

Which of them could lead to GeV or TeV gamma-ray emission?

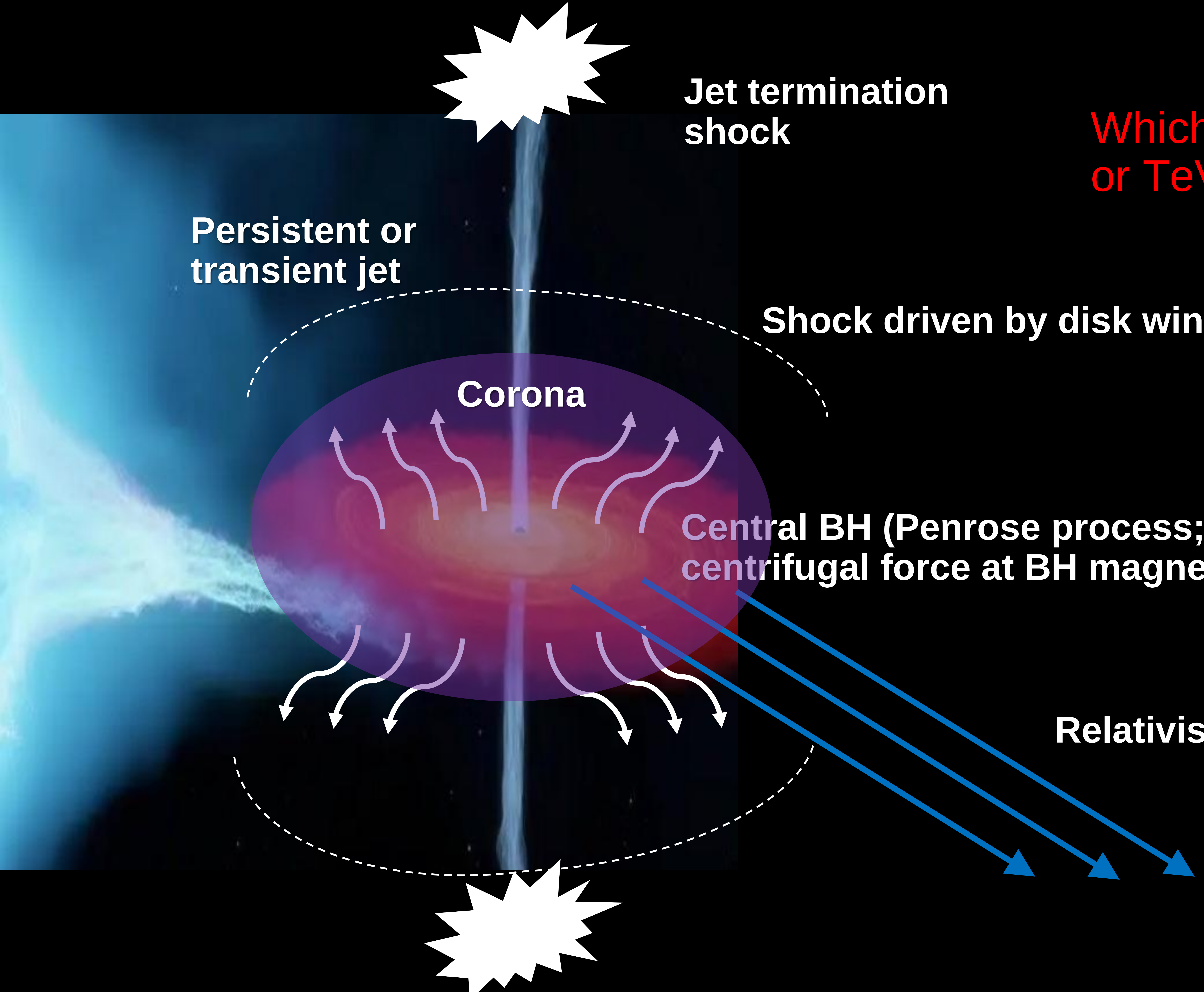

# A case study: SS 433, a very powerful Galactic microquasar

- SS 433 is a unique galactic accreting microquasar with mildly relativistic (v =0.26c), precessing jets located at a distance of 4.6 kpc

- It is composed by a compact object (10-20 $M_{sun}$ black hole) and a 30 $M_{sun}$ A7Ib supergiant star.

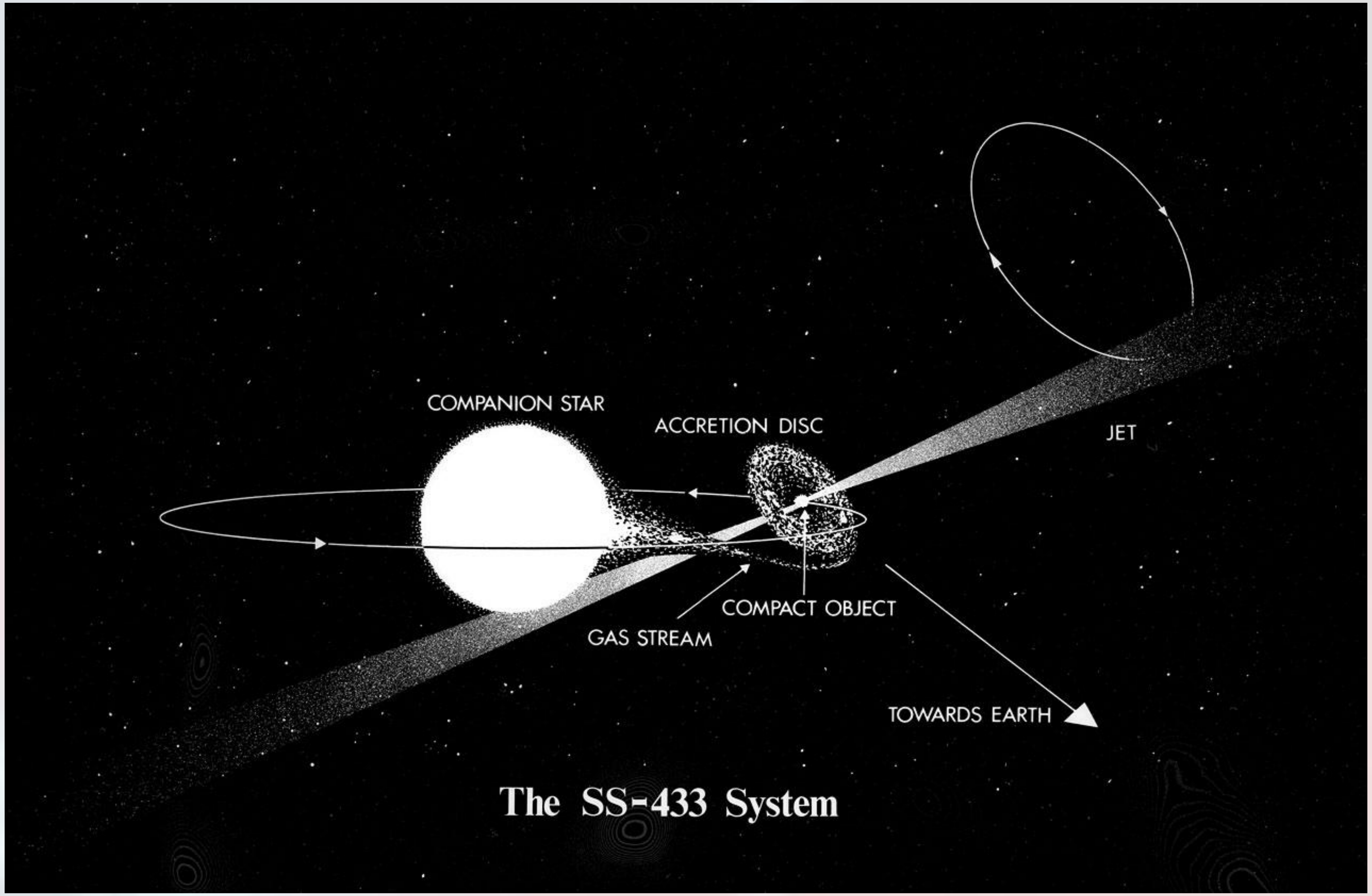


- The system exhibits photometric and spectral periodicities related to precession (~162.5 days) and orbital (13.082 days) period

# SS 433 in radio, the manatee nebula

- The jet and outflow from SS 433 leads to multi-wavelength emission and interacts with interstellar material (W50 nebula).

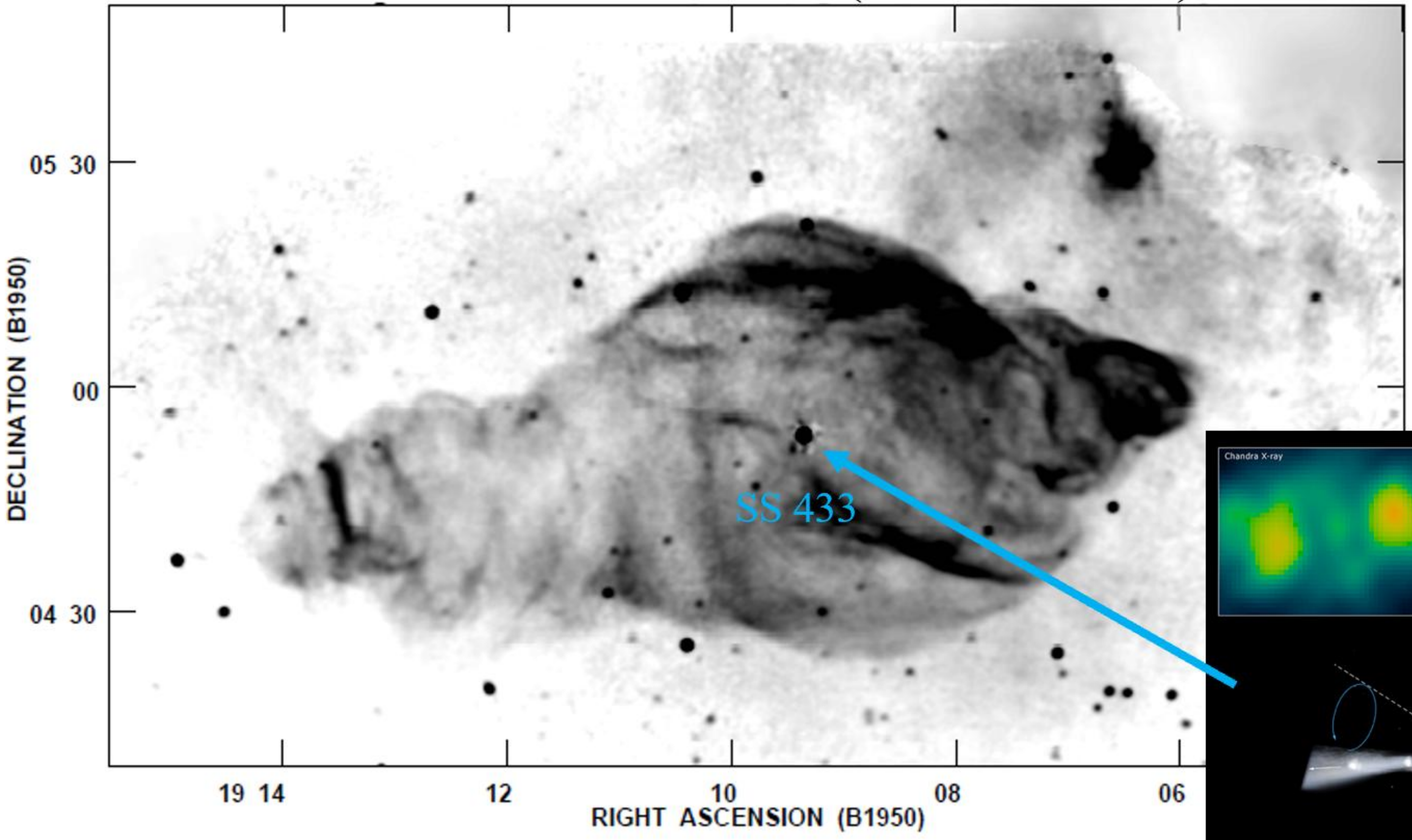


Credit: NASA/CXC/U.Amsterdam/S.Migliari et al.

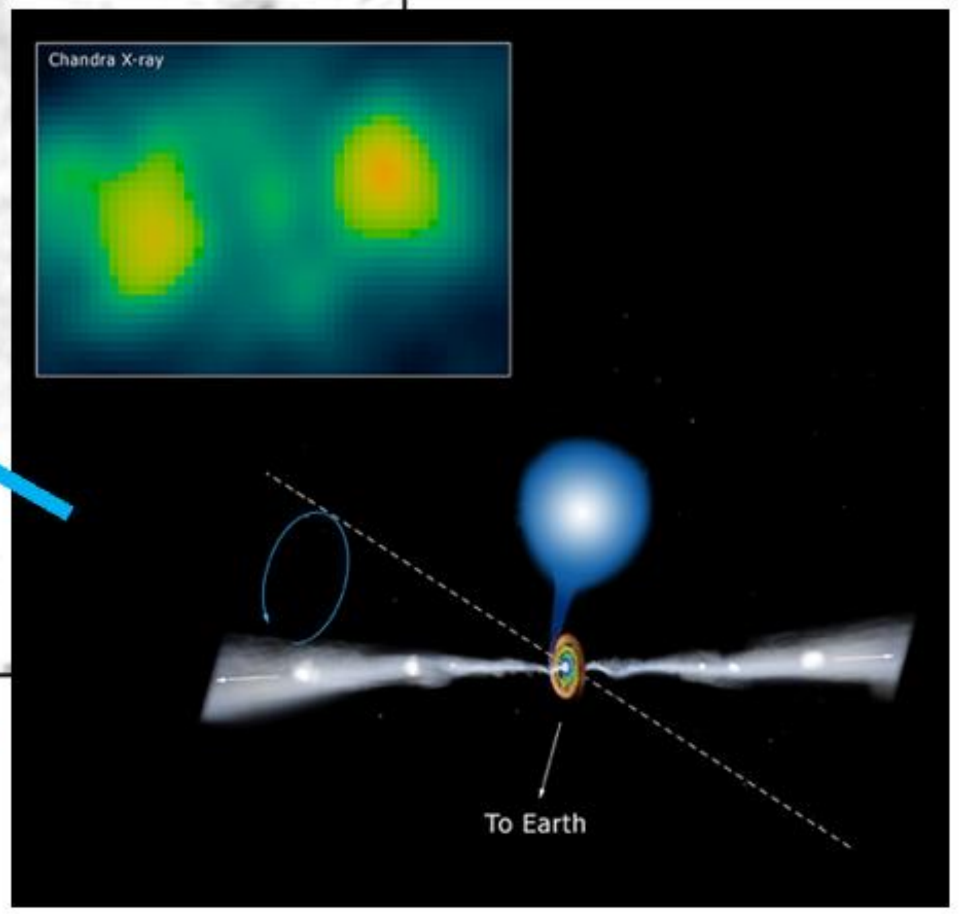


VLA radio continuum image of the W50 nebula @1465 MHz. SS 433 is at the center. Dubner et al. 1998.

# SS 433 in radio, the manatee nebula

- The jet and outflow from SS 433 leads to multi-wavelength emission and interacts with interstellar material (W50 nebula).

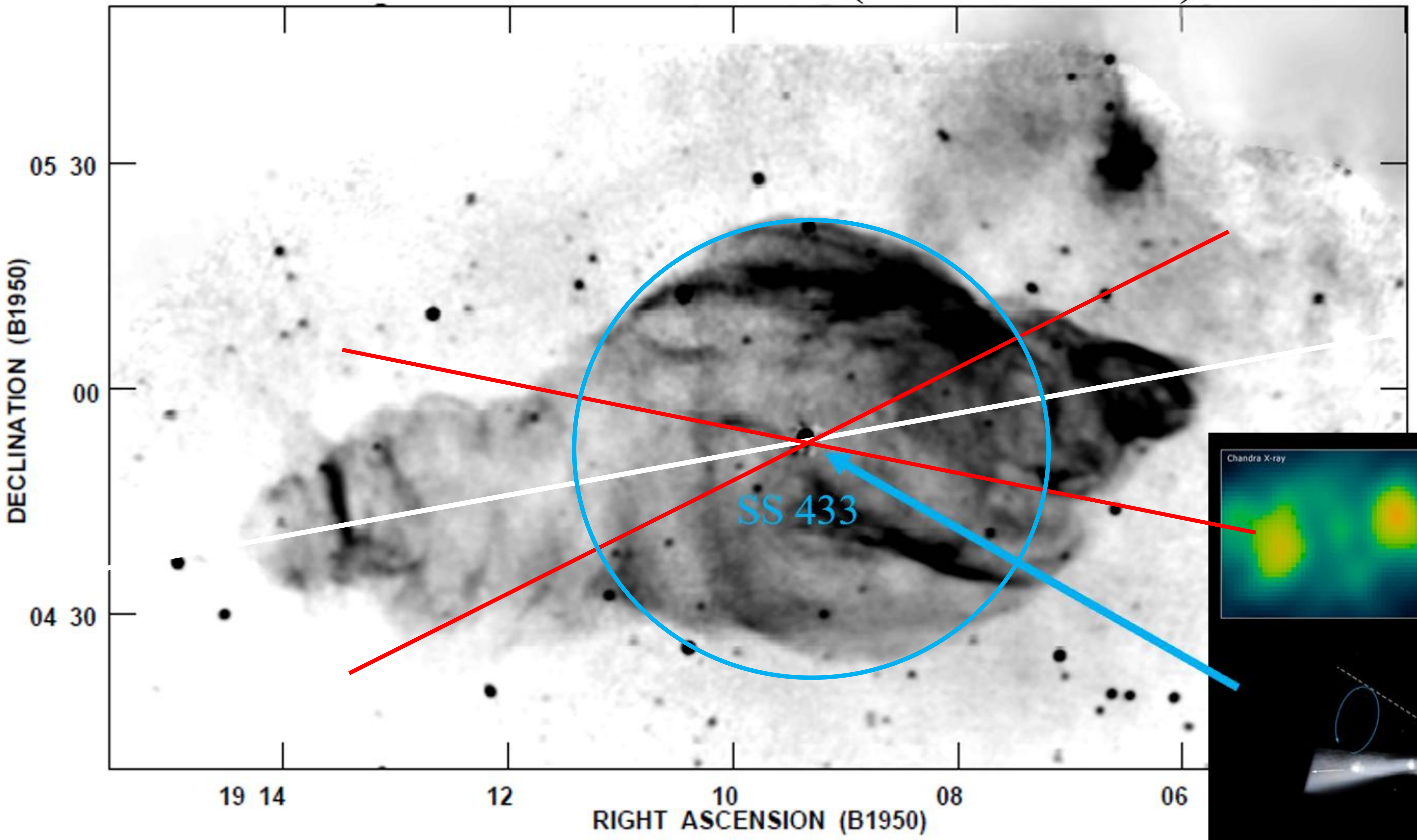


Credit: NASA/CXC/U.Amsterdam/S.Migliari et al.

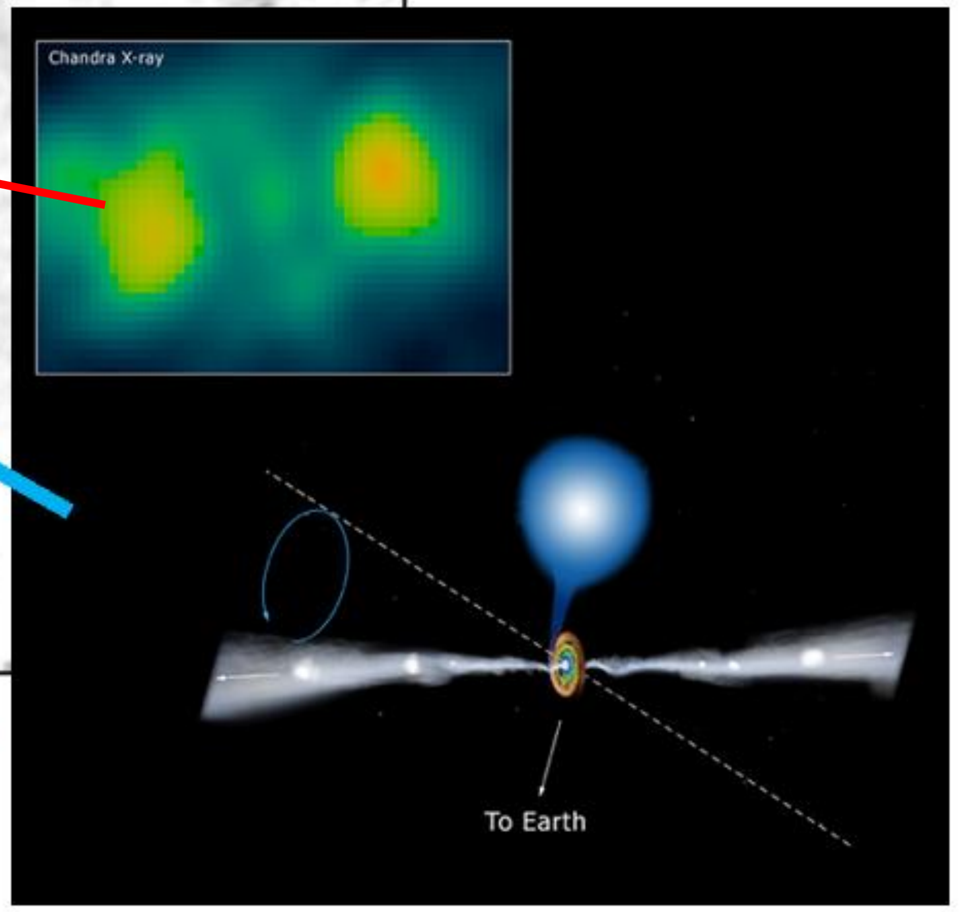


VLA radio continuum image of the W50 nebula @1465 MHz. SS 433 is at the center. Dubner et al. 1998.

# SS 433: X-ray and TeV emission from jet termination lobe

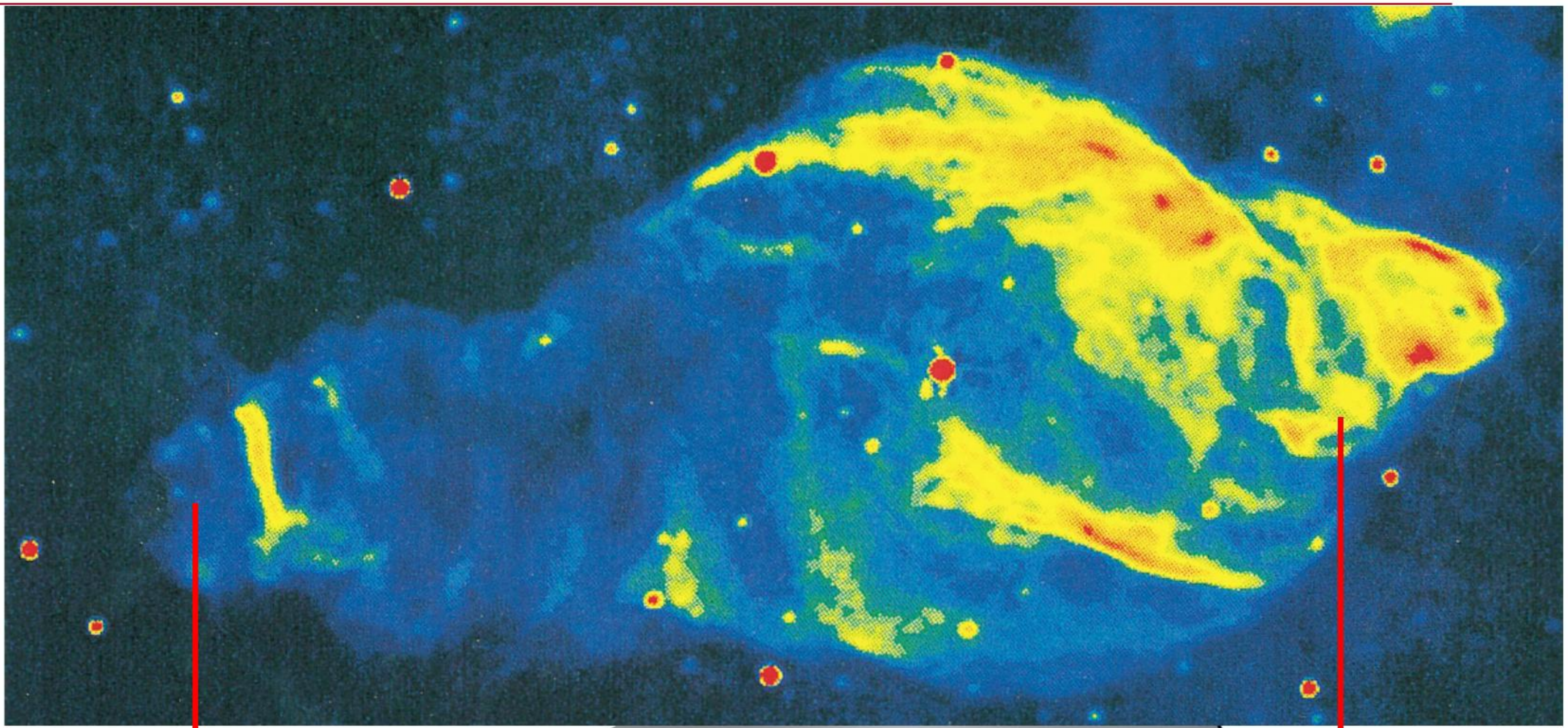

. Dubner et al. 1998.

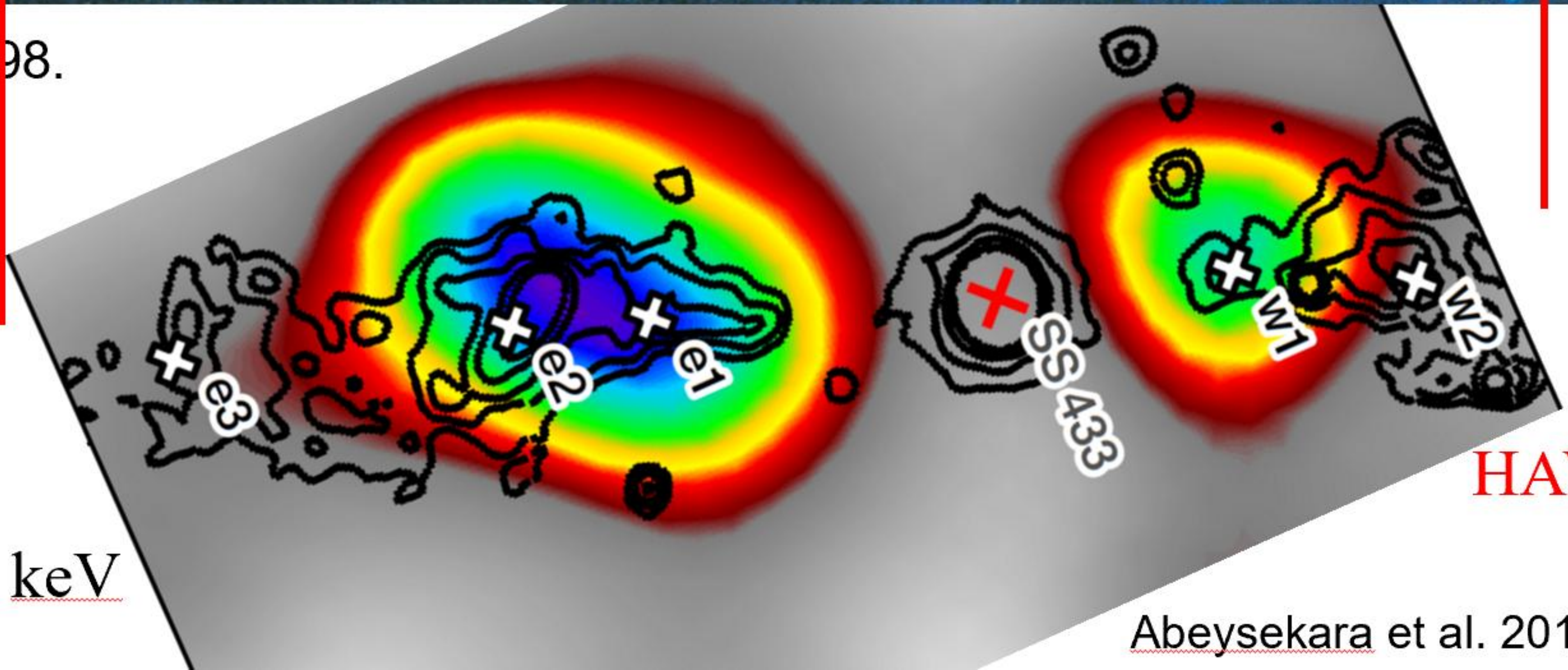


HAWC ~20 TeV

ROSAT 0.9-2 keV

Abeysekara et al. 2018, Nature

# SS 433: X-ray emission from jet termination lobe and W 50

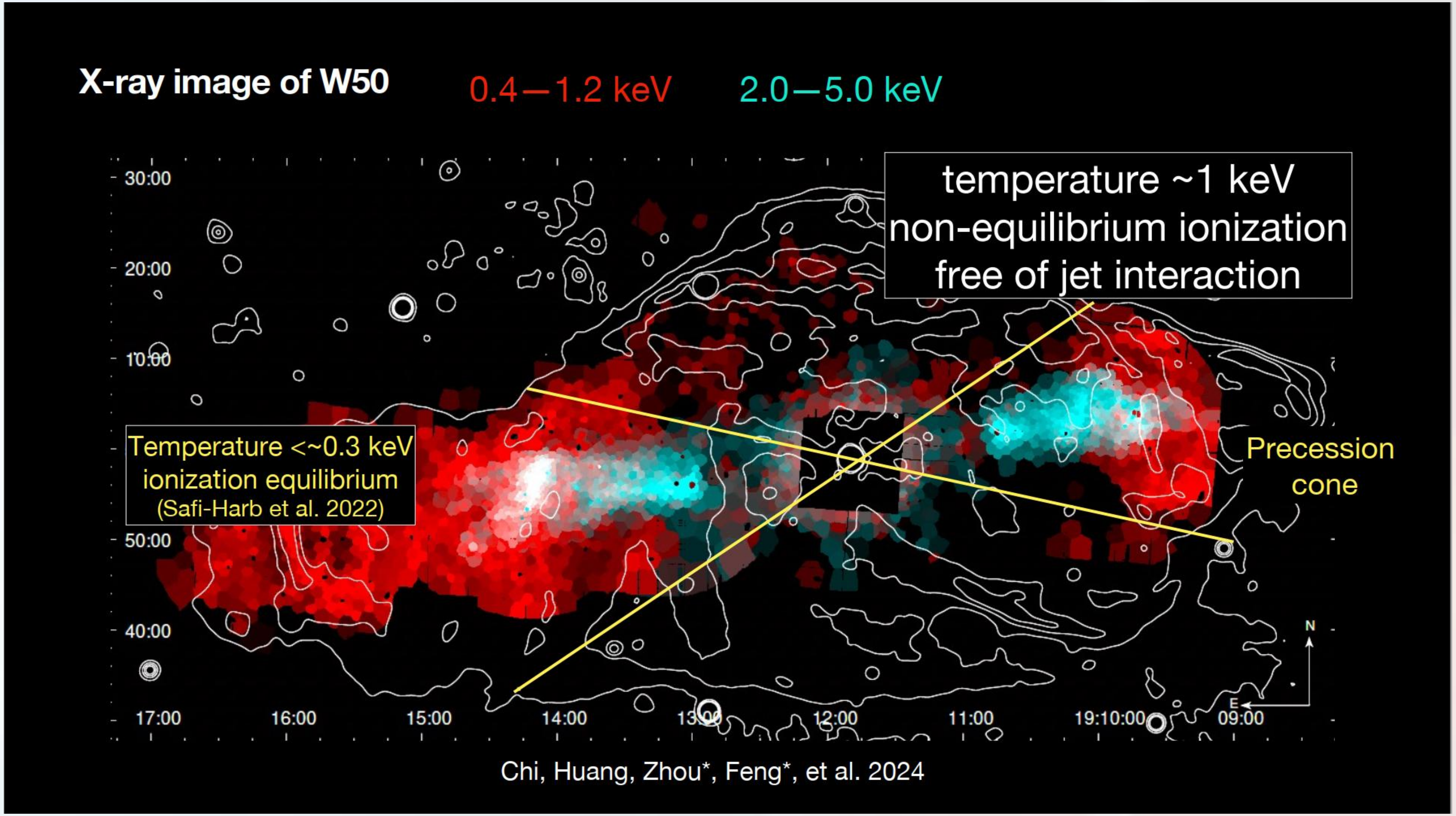


Slide from Prof. Zhou’s talk

More details see talk of Prof. Samar Safi-Harb; Chi et al. 2024

# SS 433 in multi-TeV photons (detected by HESS)

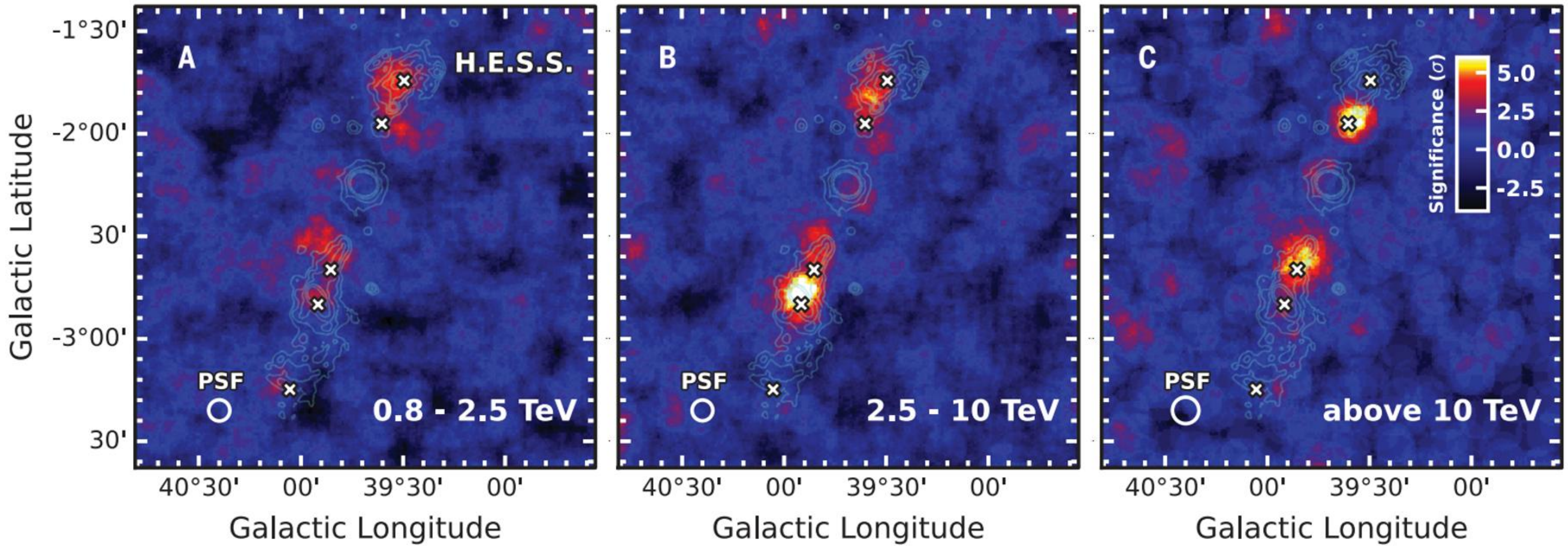


Gamma-ray observations by HESS on SS 433 in different energy bands
(HESS collaboration 2024).

HESS observation discovered an energy-dependent shift in the apparent position of the gamma-ray emission from the parsec-scale jets, indicate that inverse Compton scattering is the emission mechanism of the gamma rays.

# SS 433 seen by LHAASO—Energy dependent morphology change

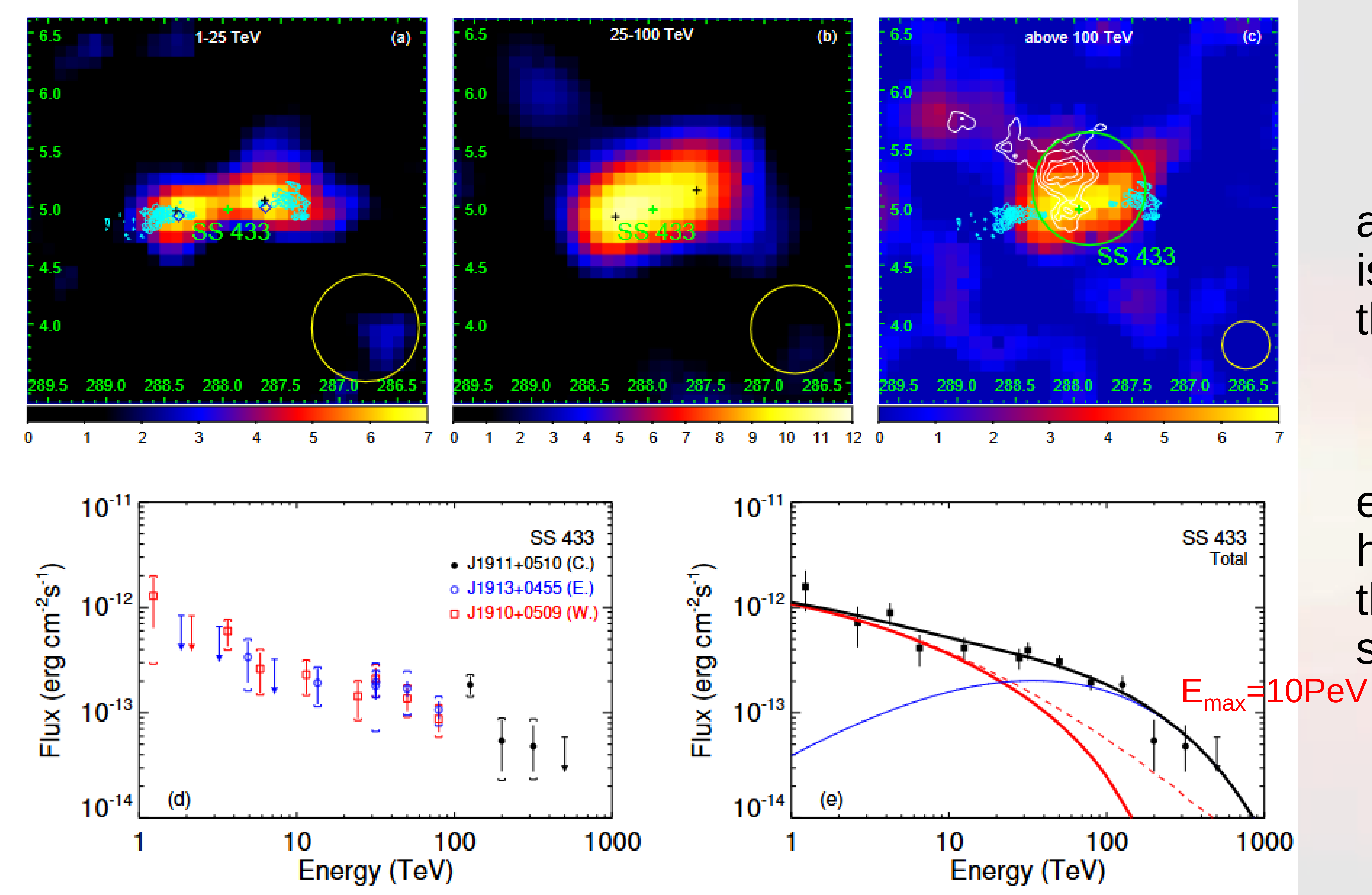


a second component is required to explain the UHE emission

either leptonic or hadronic is OK from the perspective of spectral fitting

# The possible second component

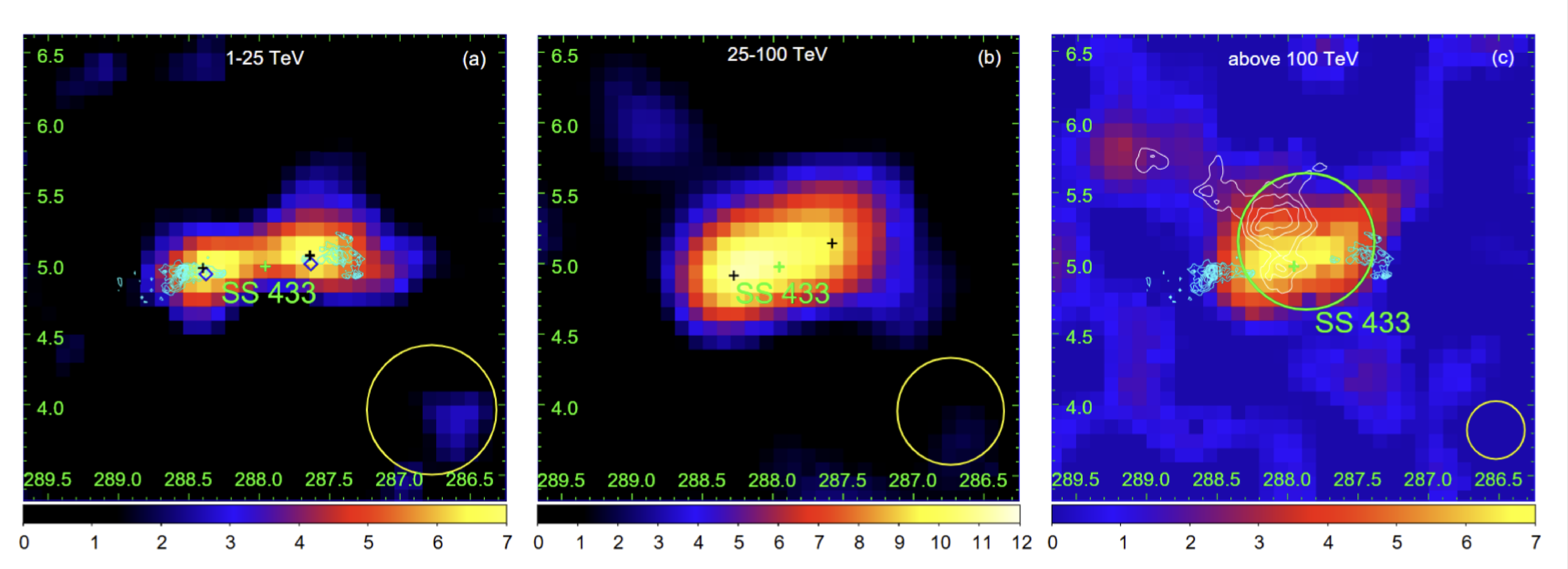


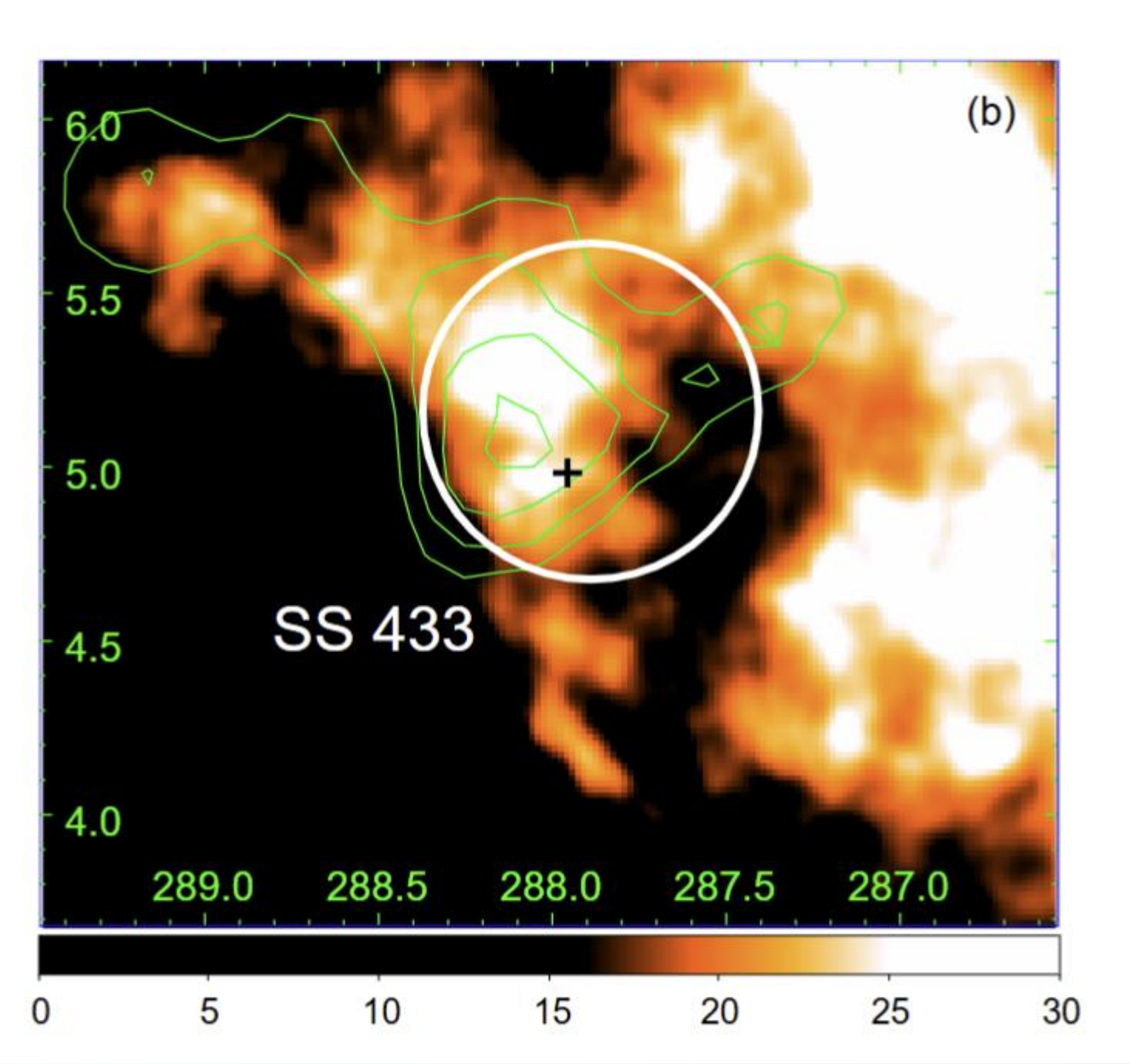


HI atomic cloud in the distance of SS 433

morphological study consistent with hadronic origin

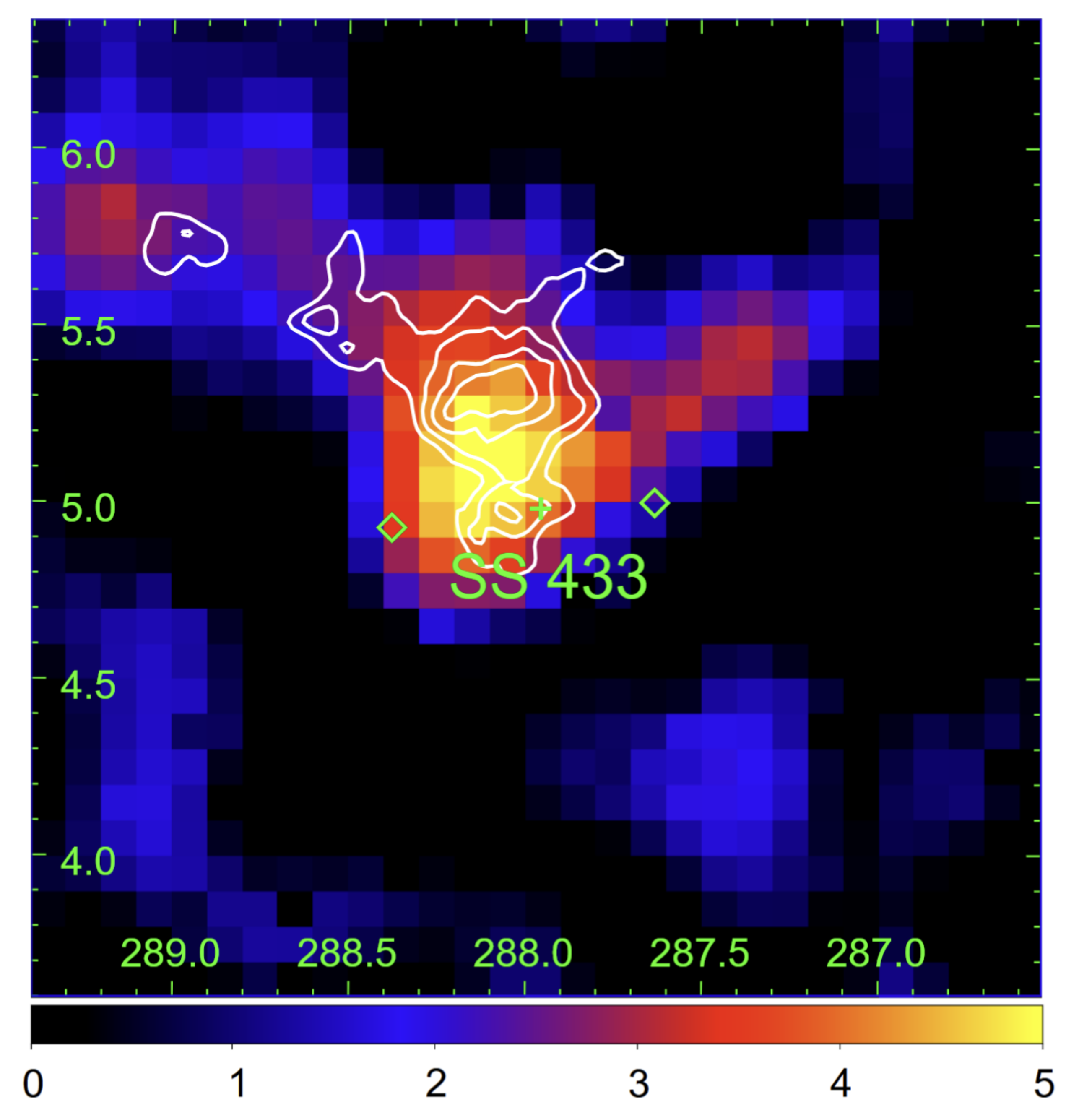


residual significance map of SS 433 region above 100 TeV after modeling jet lobe contribution

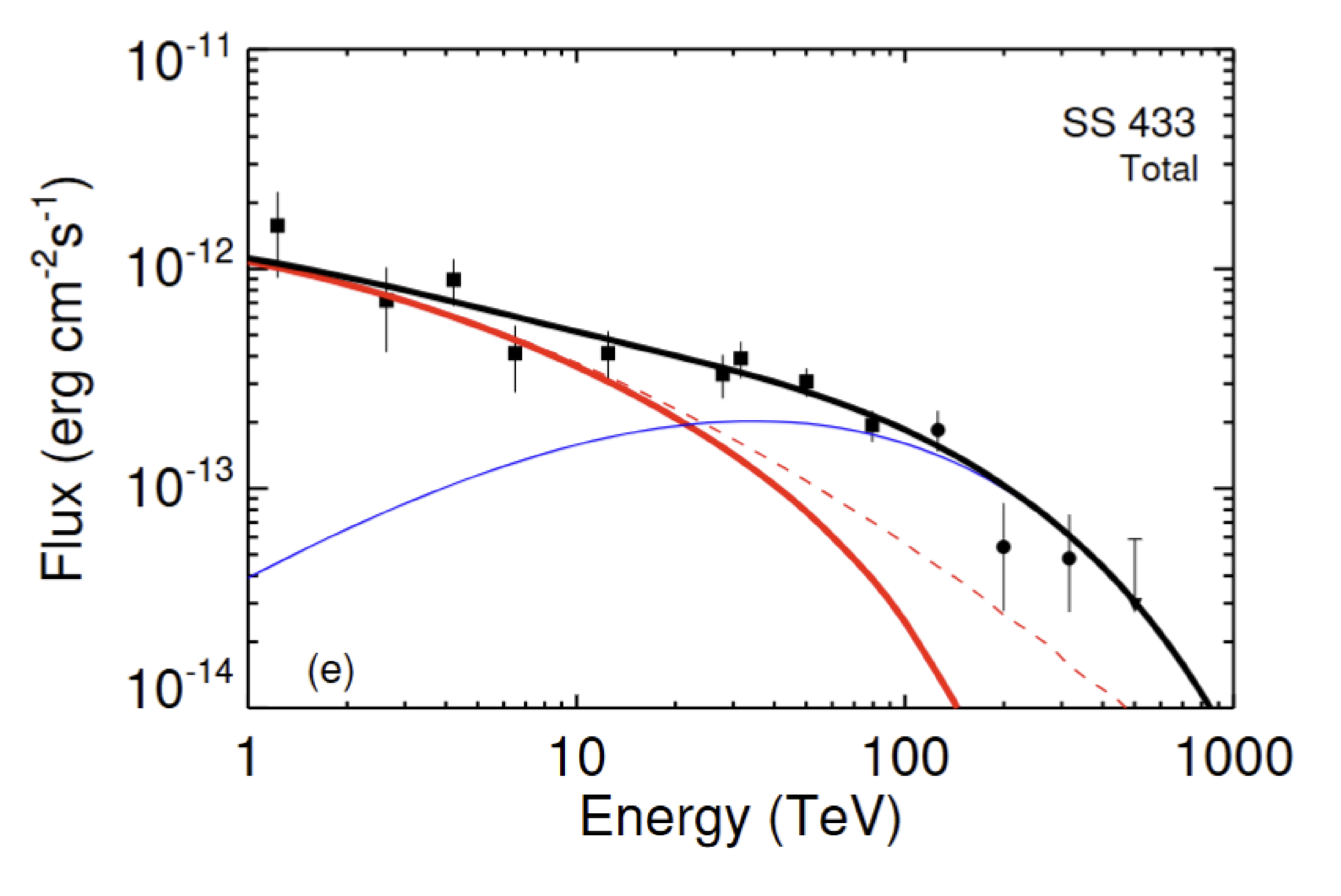


| Model of SS 433 above 100 TeV | Degree of Freedom | ΔTS | ΔAIC |
|---|---|---|---|
| 2D Gaussian | 5 | 0 | 0 |
| two-point sources at H.E.S.S. emission above 10 TeV | 4 | -8.1 | 6.1 |
| two-point sources at H.E.S.S. emission above 10 TeV + H I gas template | 6 | 10.1 | -8.1 |

Extended Data Table 1: Different models of SS 433 above 100 TeV. The ΔTS and ΔAIC are calculated regarding the 2D Gaussian model.

The significance of possible hadronic component is at ΔAIC=-8, indicating another component beyond lobes

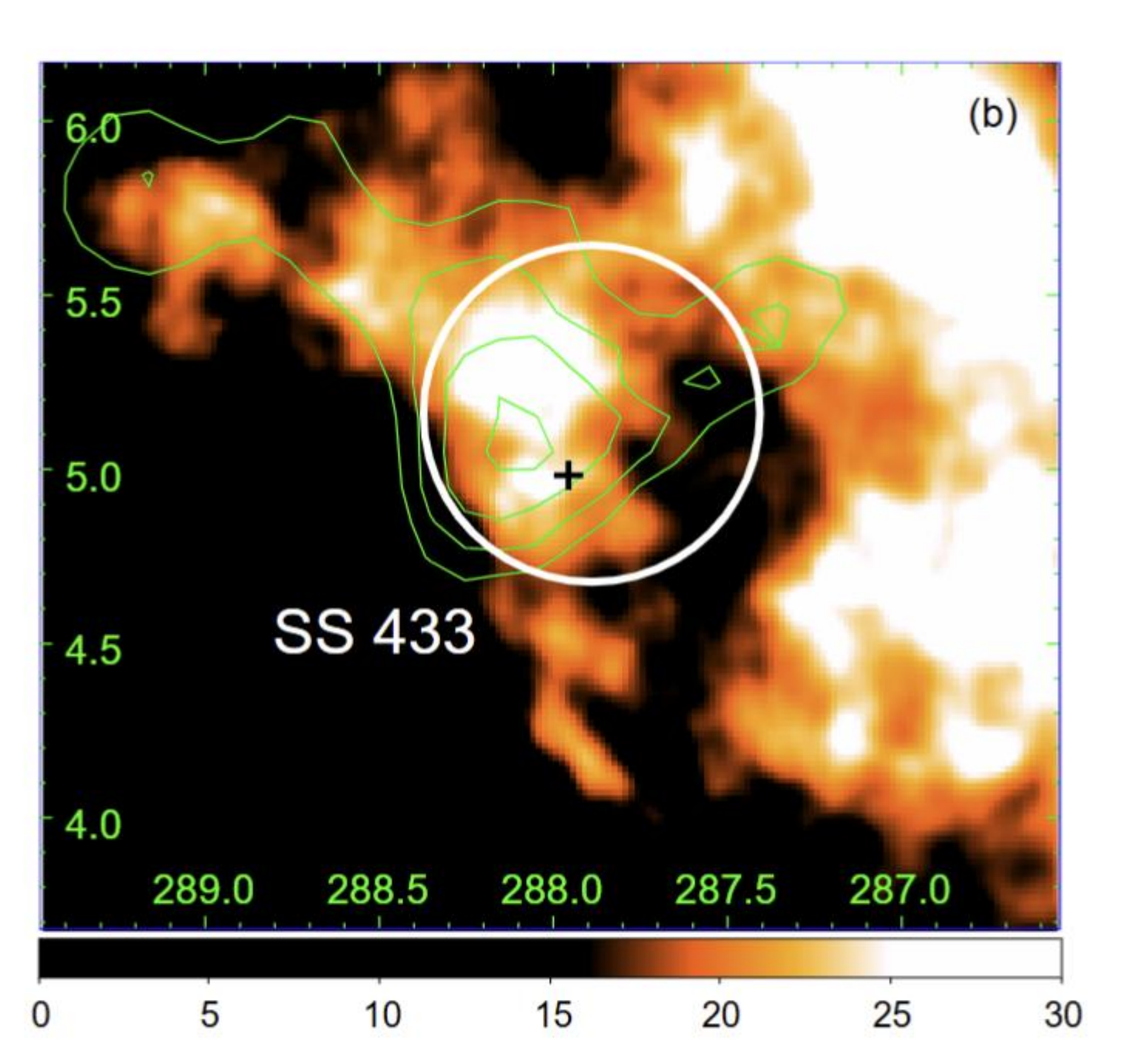


HI atomic cloud in the distance of SS 433

morphological study consistent with hadronic origin

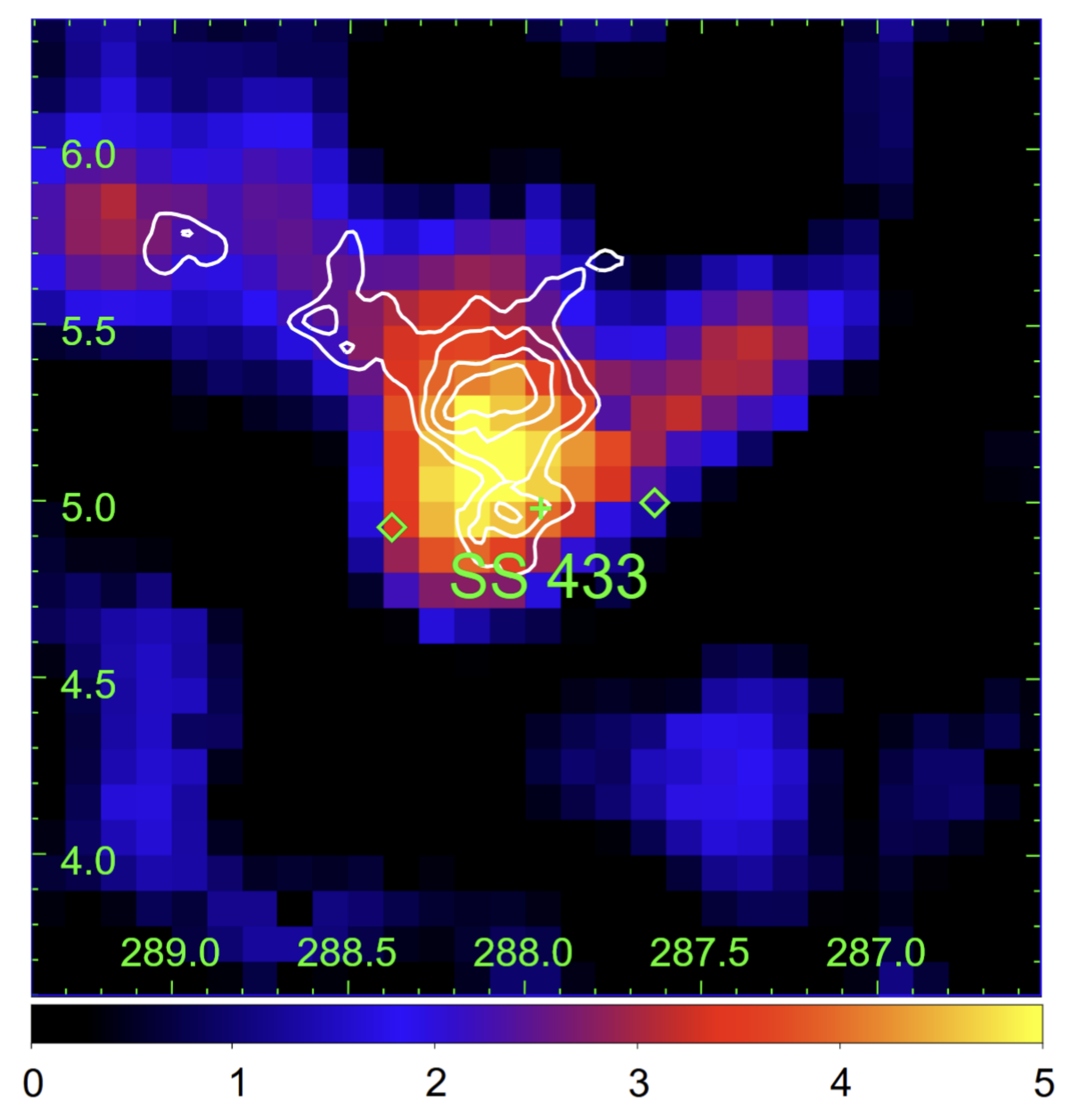


residual significance map of SS 433 region above 100 TeV after modeling jet lobe contribution


Jet termination
shock
Persistent or
transient jet
Shock driven by disk wind
Corona
Central BH (Penrose process;
centrifugal force at BH magnetosphere)
Relativistic outflow

# Another source of high energy particles: relativistic outflow

- The line-of-sight outflow velocity is 0.14-0.29c.
- Precession of the outflow in solidarity with the jet and the accretion disk, having a favorable geometry.

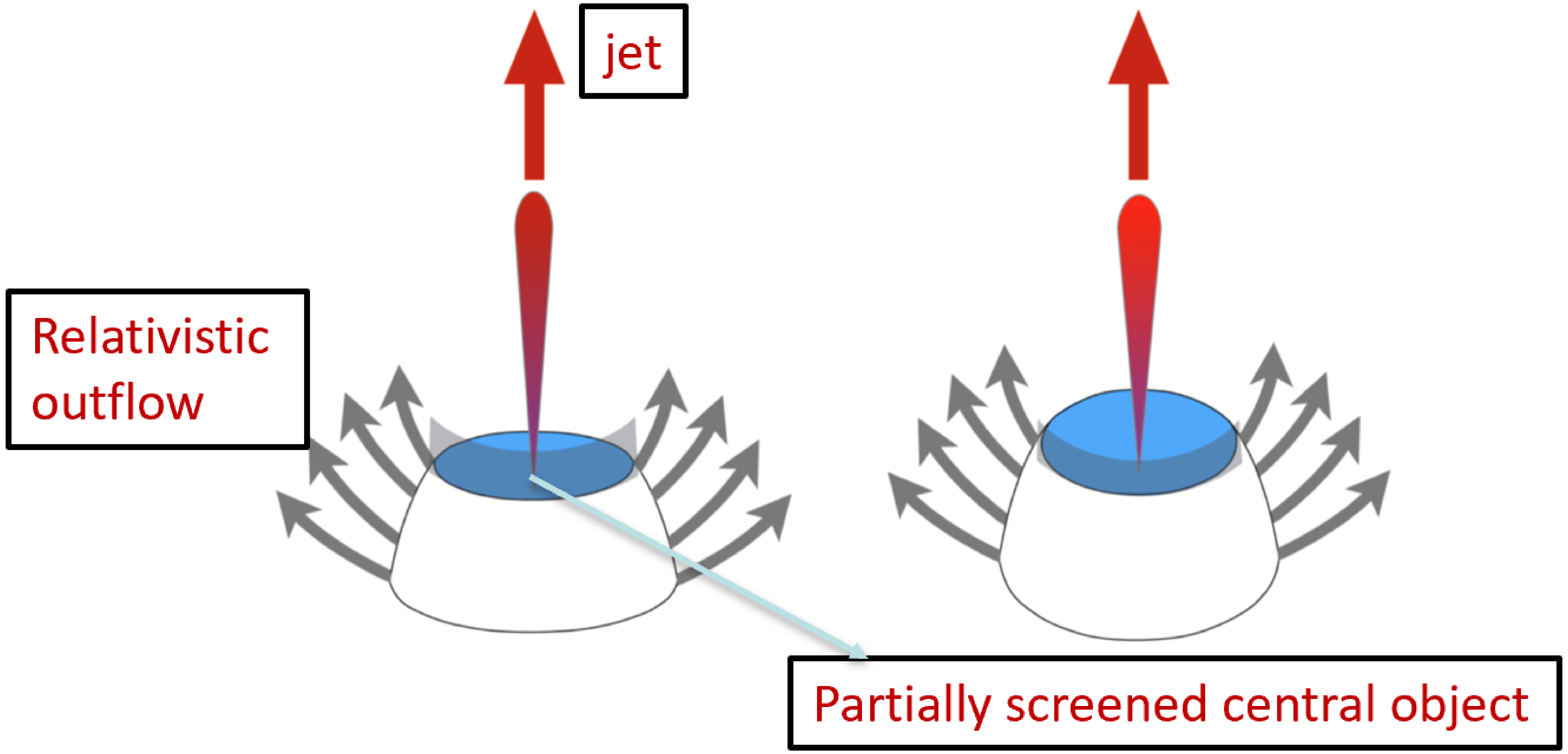


*Figure 2: Schematic of SS433 based on our observations as a function of precessional phase. In both plots, the inflated disc launches an optically thick wind (grey arrows) which also presents a screen to the X-ray bright regions within the wind-cone (blue). As the system precesses to more face-on inclinations (left to right) the jet emission (red) at soft X-rays becomes brighter due to relativistic boosting whilst the reflected flux increases with the visible area of the open wind-cone[27].*

Middleton et al. 2018, 2021

# SS 433 in GeV

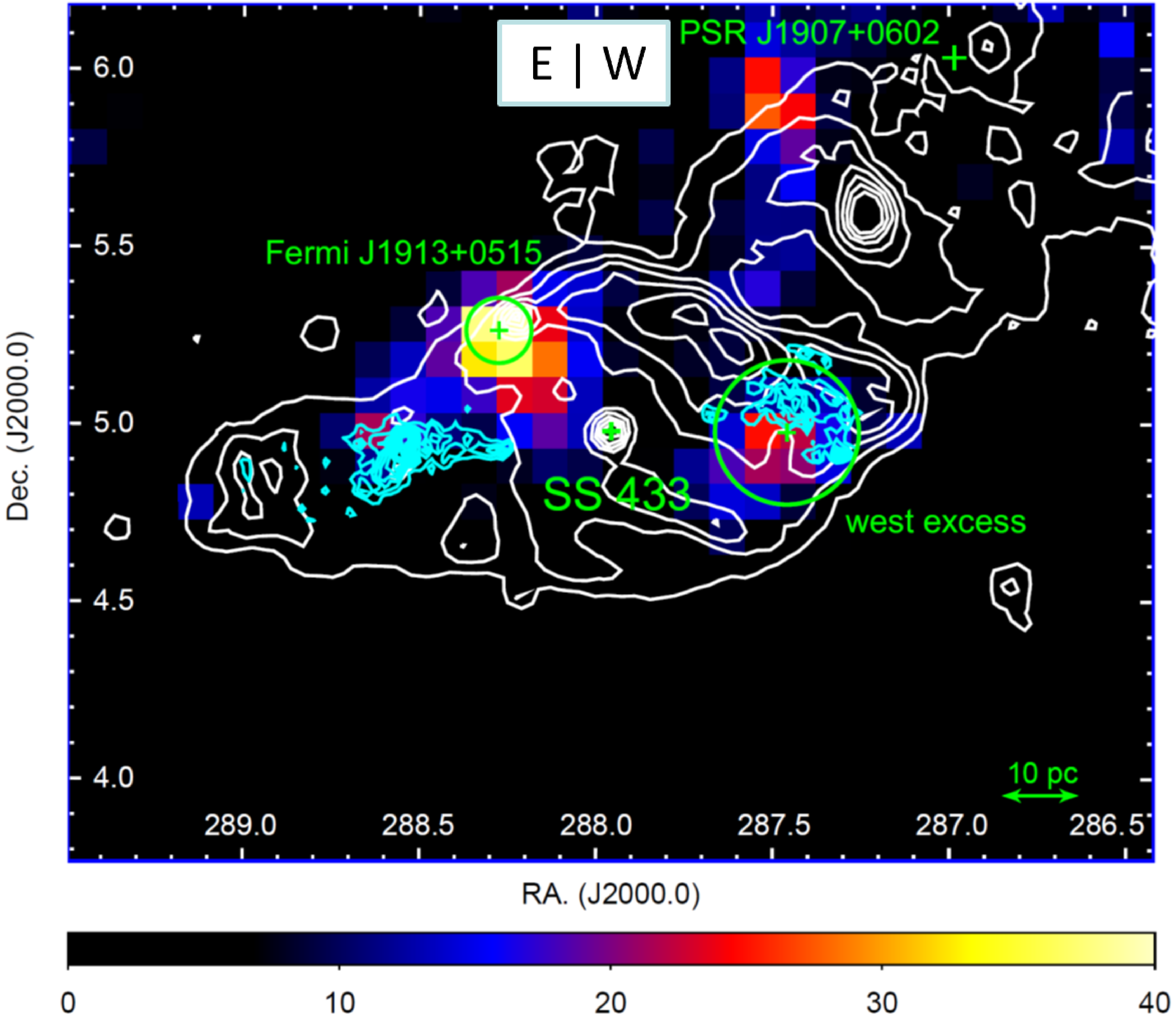


TS map
(1-300 GeV off-peak phase of PSR J1907+0602)

White contour is Effelsberg 11cm radio continuum (2695 MHz) while cyan contour is X-ray ROSAT observation in 0.9-2 keV.

Two regions of TS excesses are apparent in the map.

The west excess location is consistent with the one found in X-rays. Not the east one.

Li et al. 2020, NA, 4, 1177

# The periodicity hint is confirmed by likelihood analysis

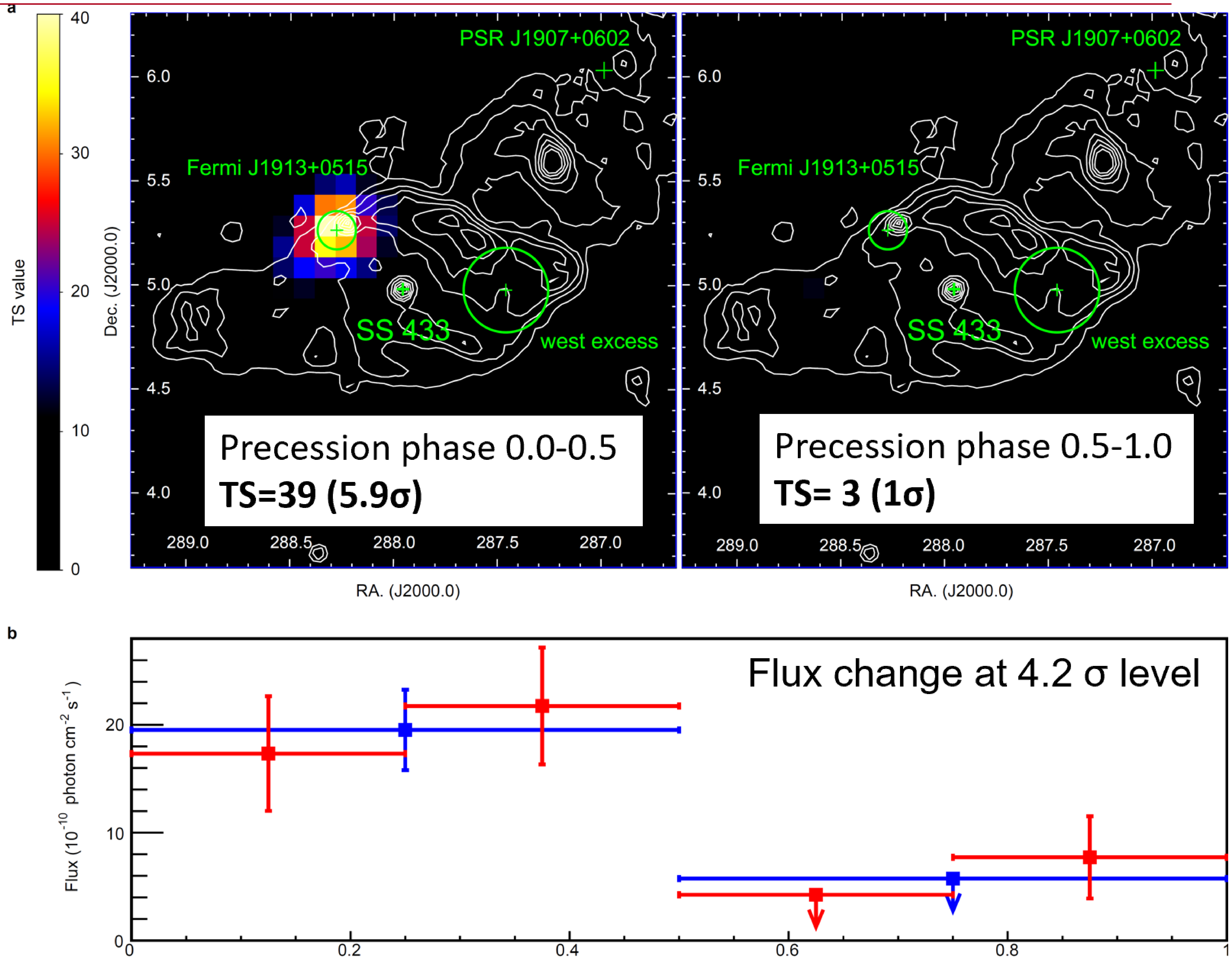

# The position of the timing excess is off the center and the jets' path

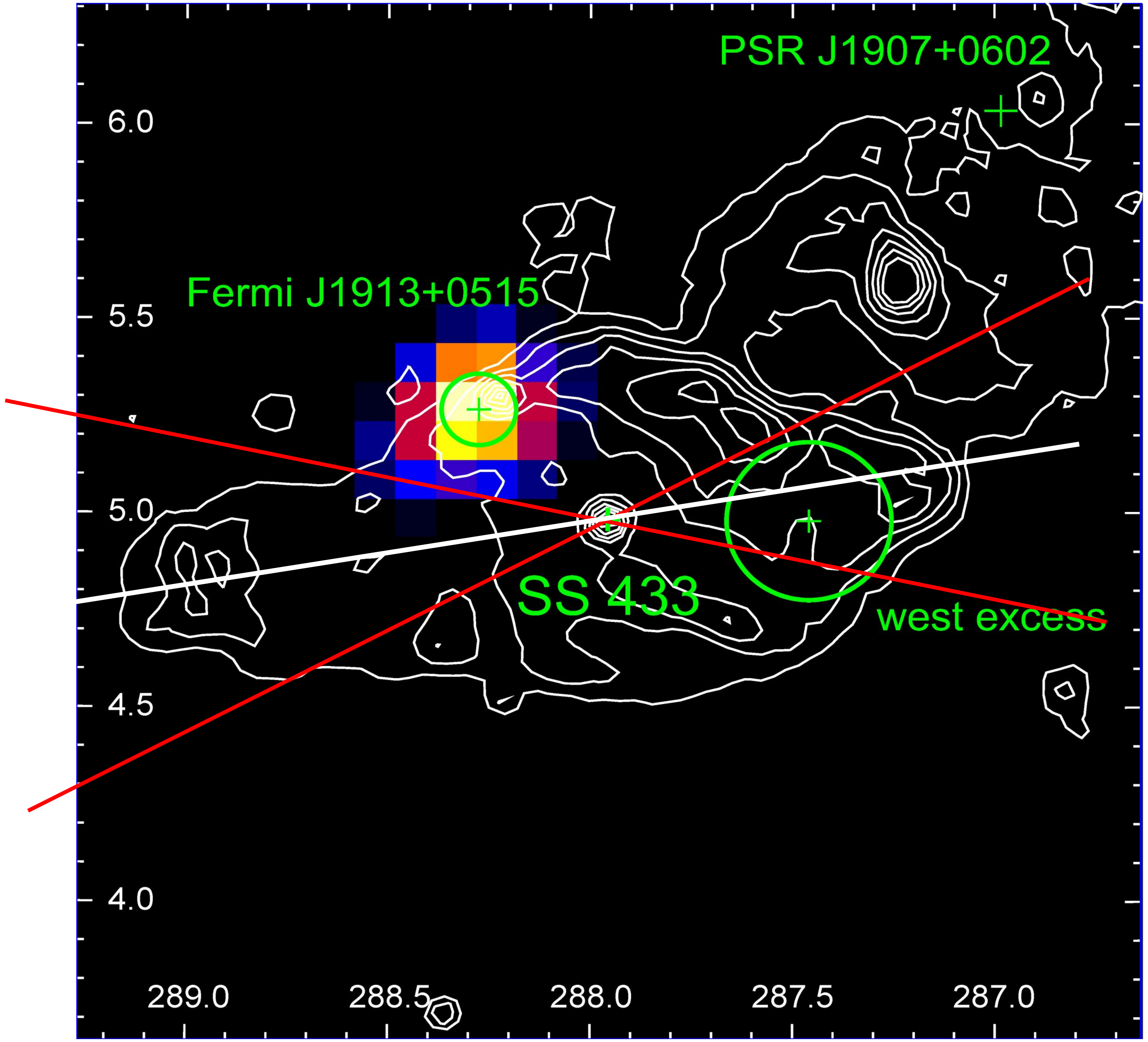


The projected distance between GeV excess and SS 433 is ~35pc

# The only notable thing at the location of the excess is a cloud

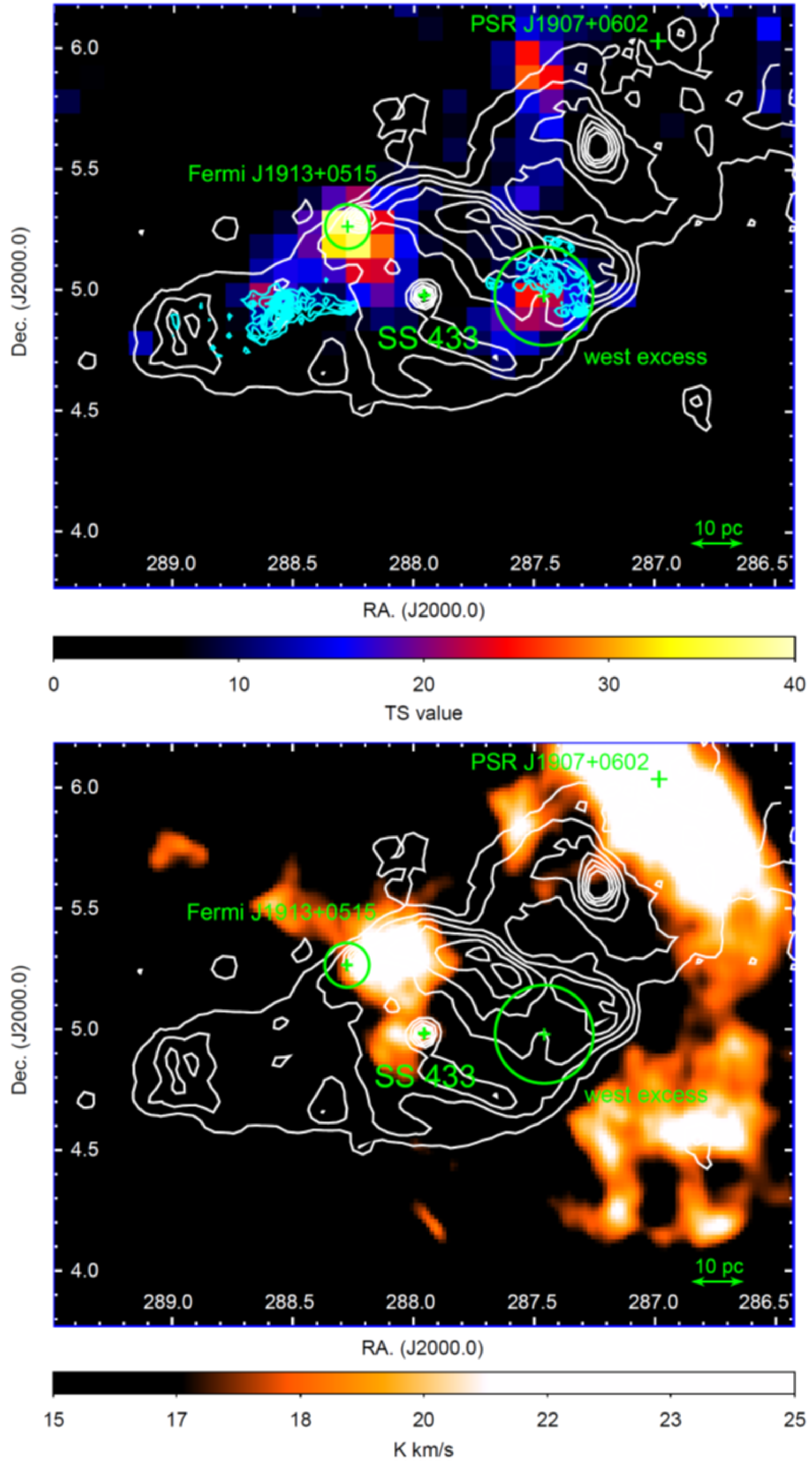


Arecibo HI emission integrated in the interval 65-82 km $s^{-1}$.

The image has been scaled by *sin* |*b*| (*b* is Galactic latitude) to enhance the features far from the Galactic plane.

# SS 433 in GeV: cloud heart-beating via anisotropic diffusion?

IRAM 12CO (1-0) and 12CO (2-1) map in 70-73 km/s, the distance consistent with SS 433 (Li et al. 2025, in prep.)

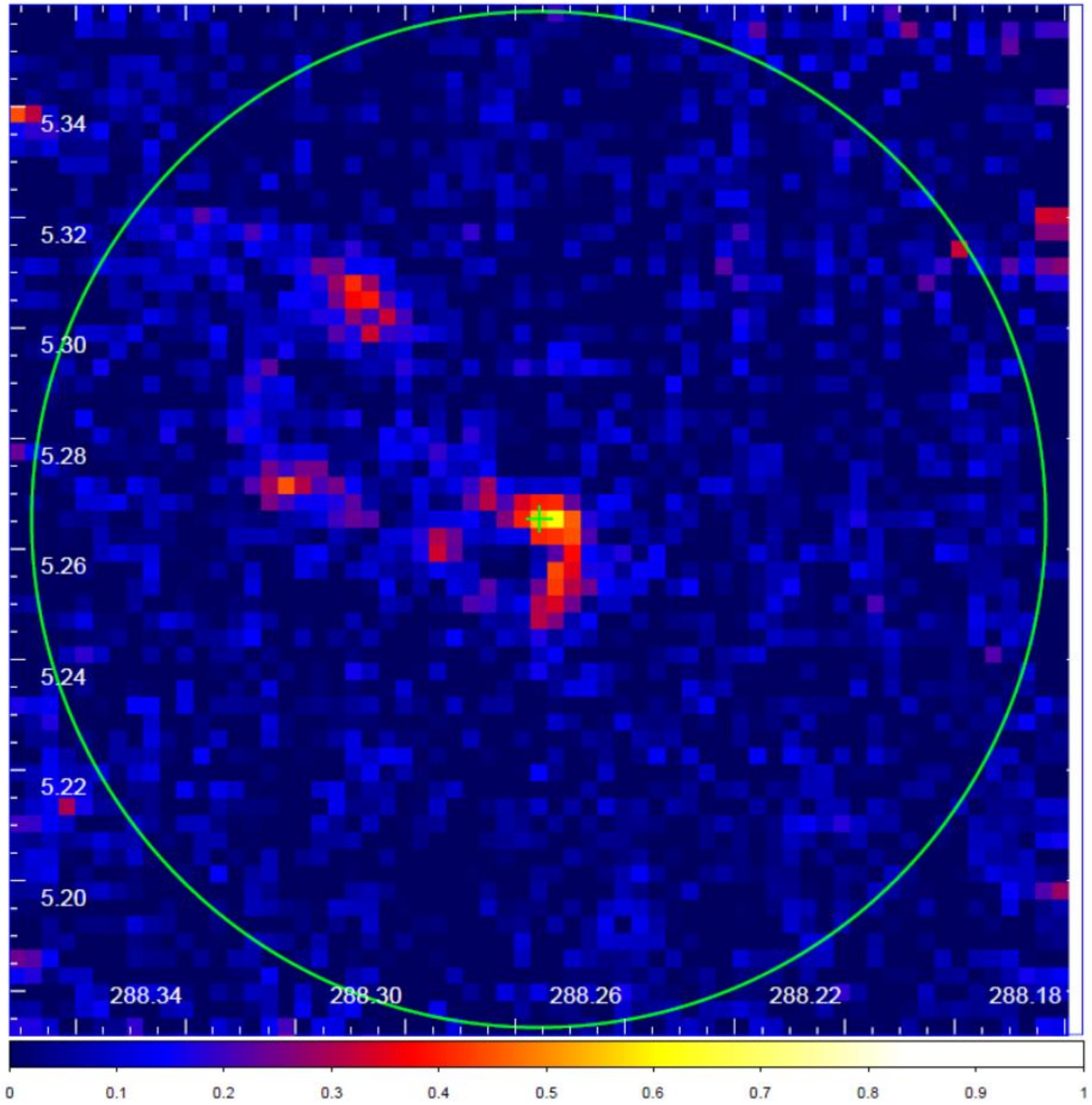


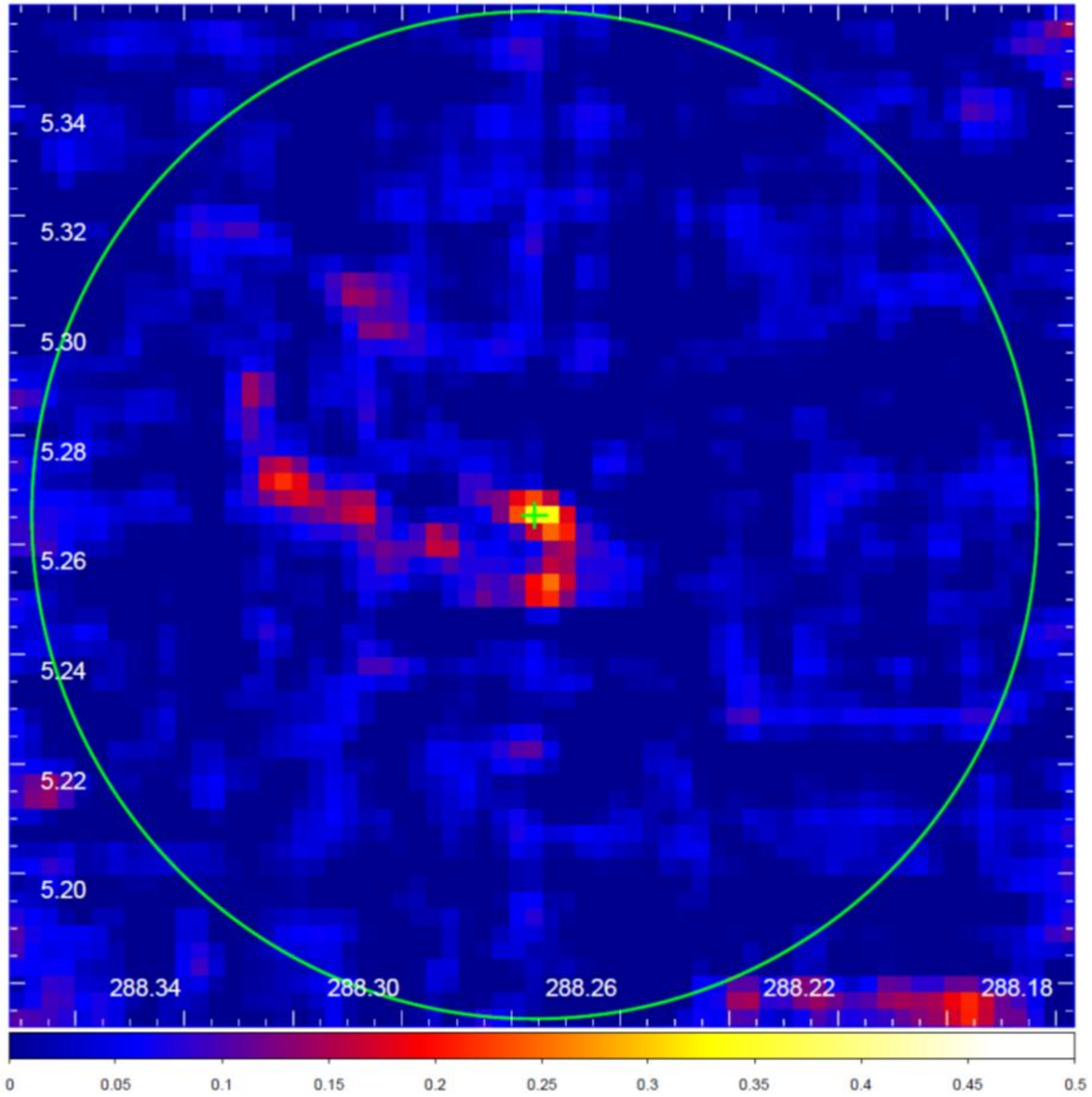

# SS 433 in GeV: cloud heart-beating via anisotropic diffusion?

Chandra image in 0.3-10 keV (Li et al. 2025, in prep)

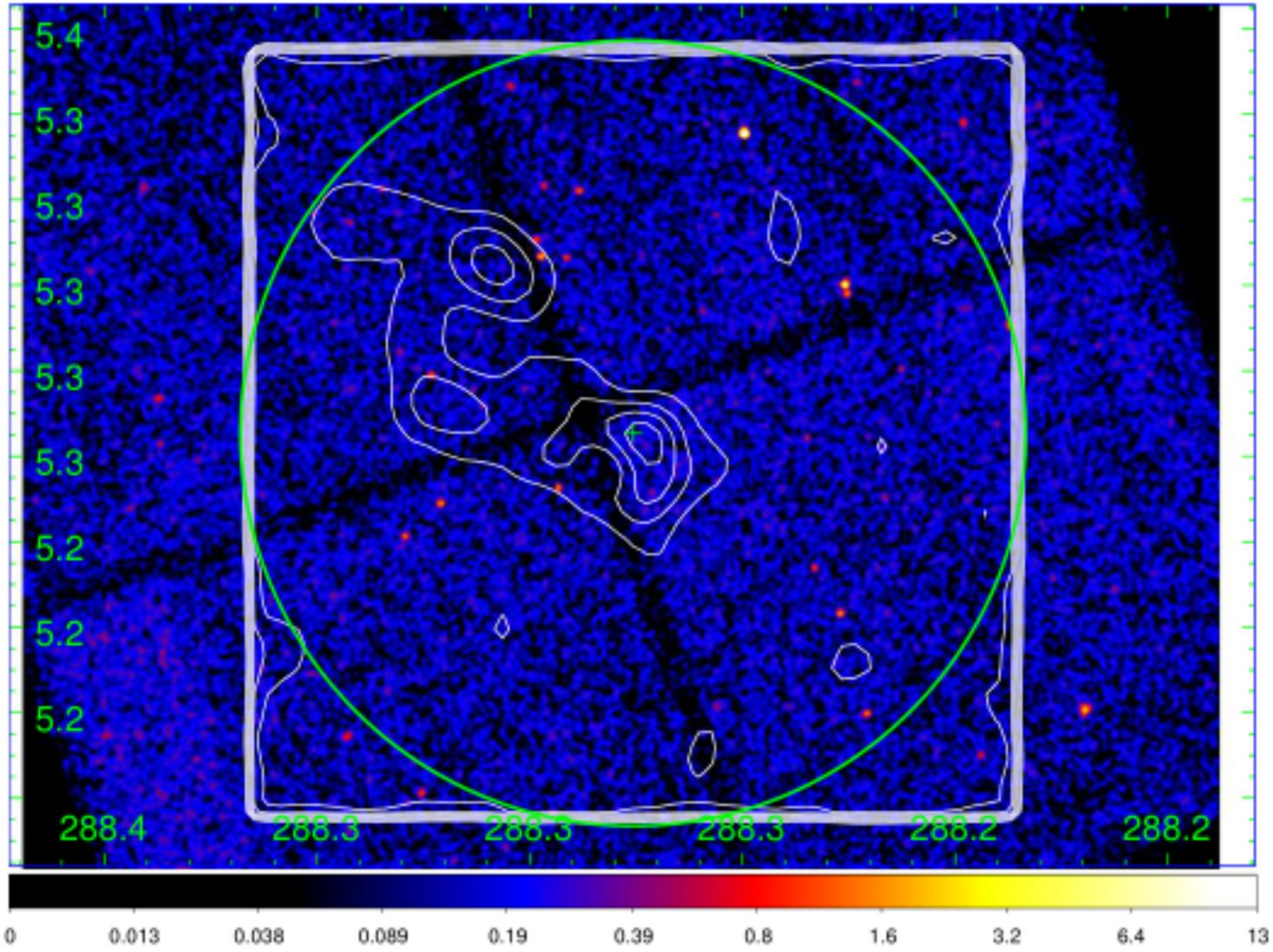

# Jet

relativistic outflow

# SS 433

Particle acceleration from jet and relativistic outflow

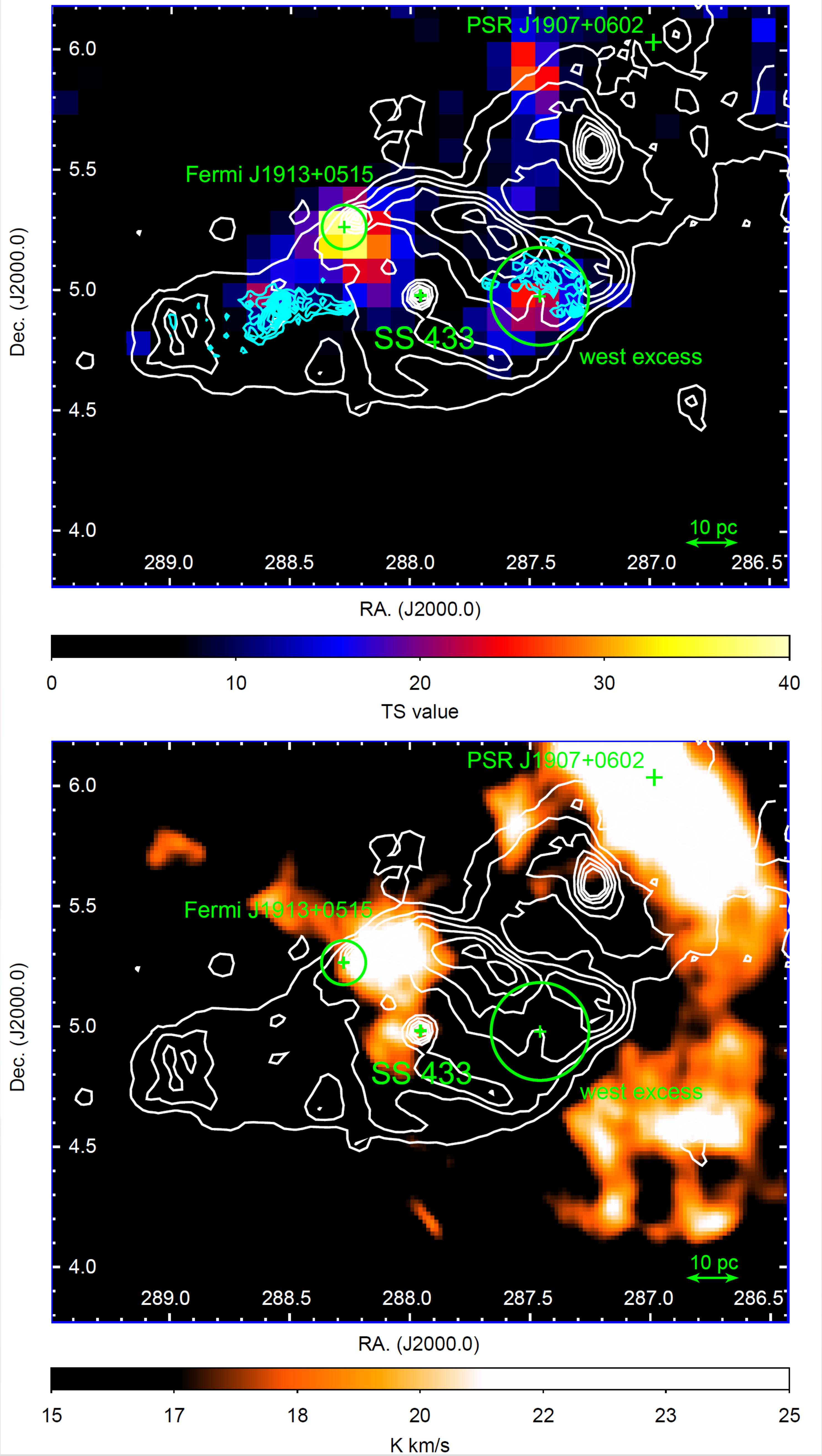


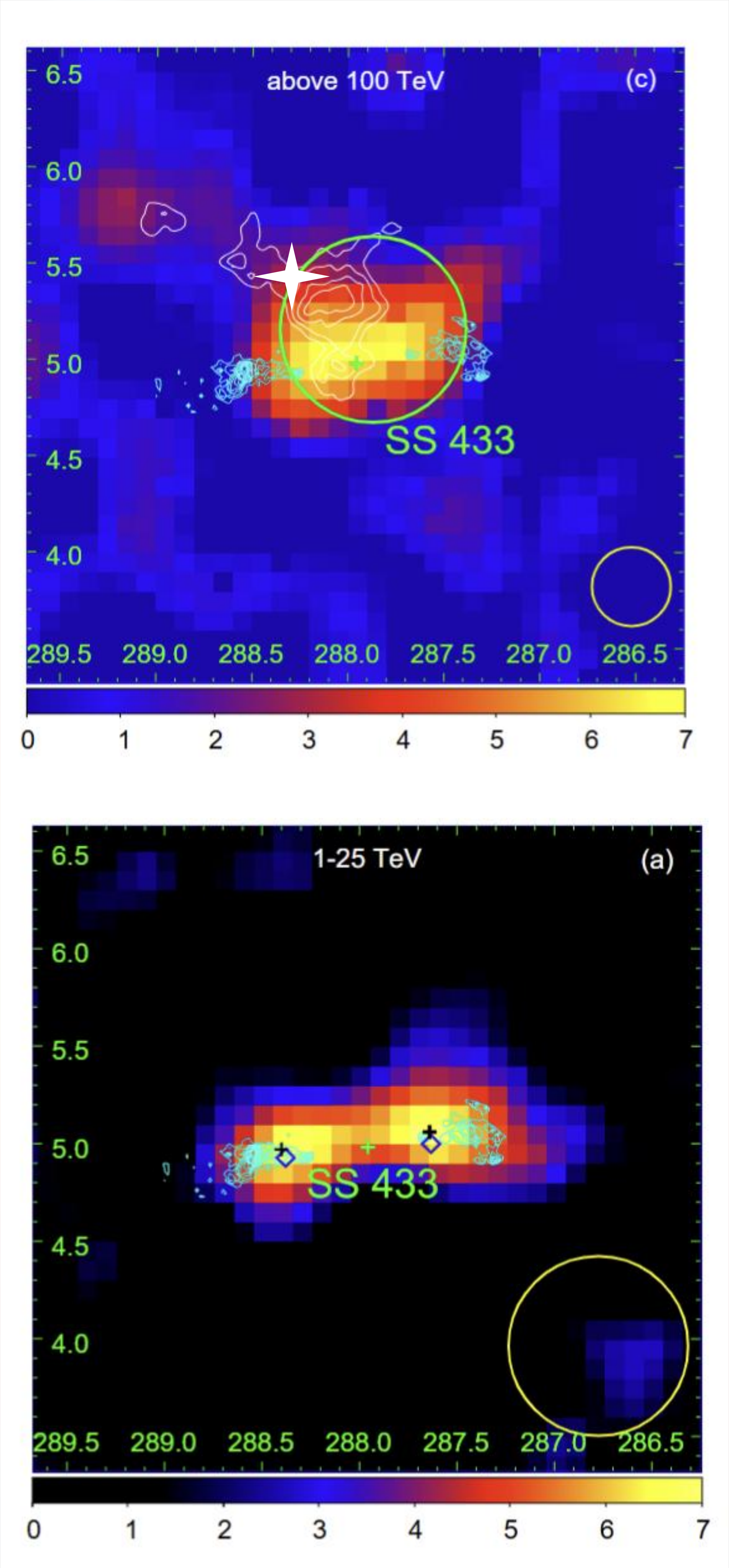

# Relativistic outflow in supermassive blackholes

In supermassive blackholes, ultra fast outflows (v>0.1c) could produce gamma-ray emission, by the cosmic rays (CRs) accelerated at the shock front.

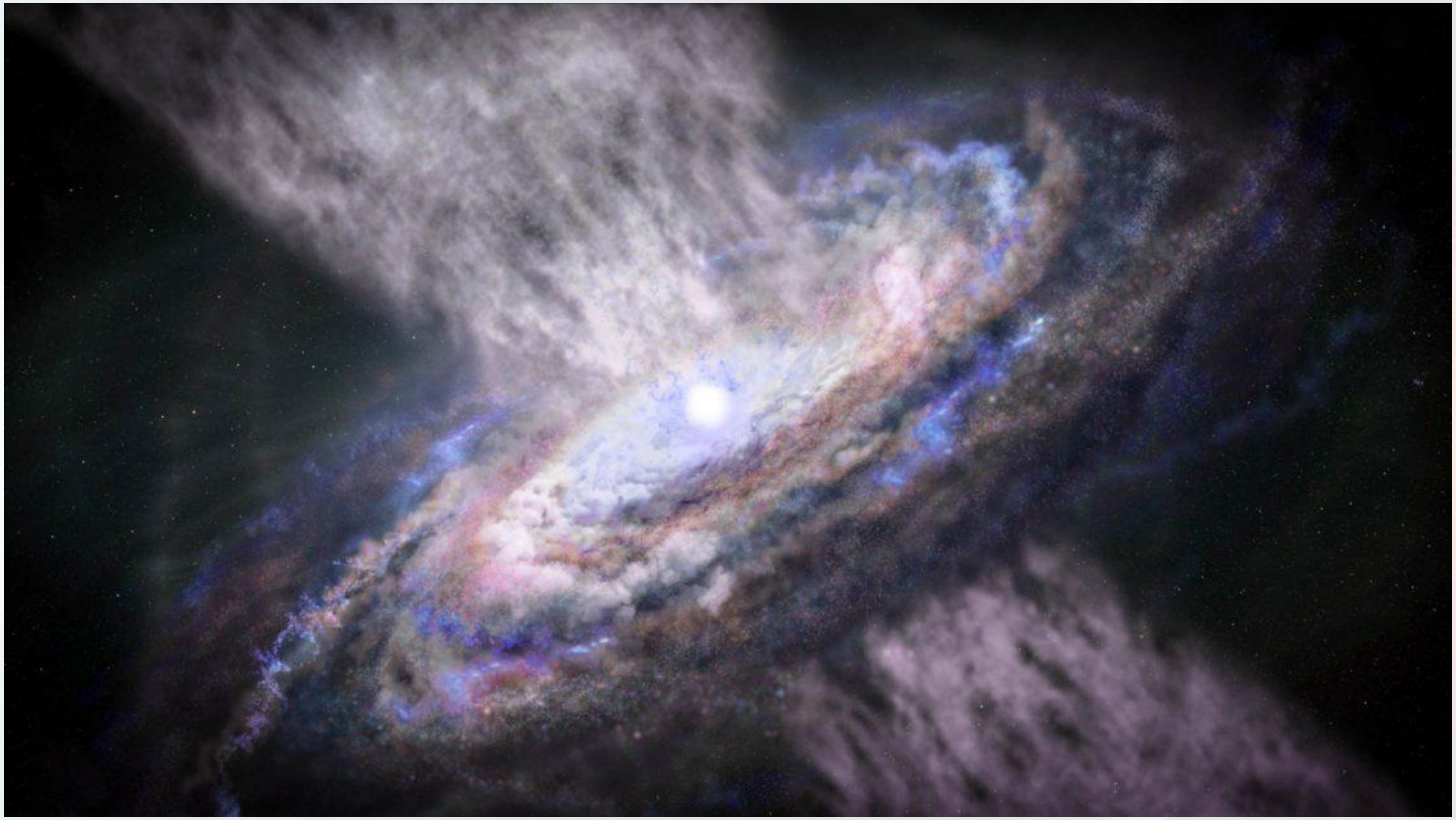

# Relativistic outflow in supermassive blackholes

In supermassive blackholes, ultra fast outflows (v>0.1c) could produce gamma-ray emission, by the cosmic rays (CRs) accelerated at the shock front.

The Astrophysical Journal, 921:144 (14pp), 2021 November 10 https://doi.org/10.3847/1538-4357/ac1bb2


CrossMark

## Gamma Rays from Fast Black-hole Winds

M. Ajello[1], L. Baldini[2], J. Ballet[3], G. Barbiellini[4,5], D. Bastieri[6,7], R. Bellazzini[8], A. Berretta[9], E. Bissaldi[10,11], R. D. Blandford[12], E. D. Bloom[12], R. Bonino[13,14], P. Bruel[15], S. Buson[16], R. A. Cameron[12], D. Caprioli[17], R. Caputo[18], E. Cavazzuti[19], G. Chartas[20], S. Chen[6,21], C. C. Cheung[22], G. Chiaro[23], D. Costantin[24], S. Cutini[25], F. D'Ammando[26], P. de la Torre Luque[10], F. de Palma[27,28], A. Desai[29], R. Diesing[17], N. Di Lalla[12], F. Dirirsa[30], L. Di Venere[10,11], A. Domínguez[31], S. J. Fegan[15], A. Franckowiak[32], Y. Fukazawa[33], S. Funk[34], P. Fusco[10,11], F. Gargano[11], D. Gasparrini[35,36], N. Giglietto[10,11], F. Giordano[10,11], M. Giroletti[26], D. Green[37], I. A. Grenier[3], S. Guiriec[18,38], D. Hartmann[1], D. Horan[15], G. Jóhannesson[39,40], C. Karwin[1], M. Kerr[22], M. Kovačević[25], M. Kuss[8], S. Larsson[41,42,43], L. Latronico[13], M. Lemoine-Goumard[44], J. Li[45], I. Liodakis[46], F. Longo[4,5], F. Loparco[10,11], M. N. Lovellette[22], P. Lubrano[25], S. Maldera[13], A. Manfreda[2], S. Marchesi[47], L. Marcotulli[1], G. Martí-Devesa[48],

Ajello et al. 2021

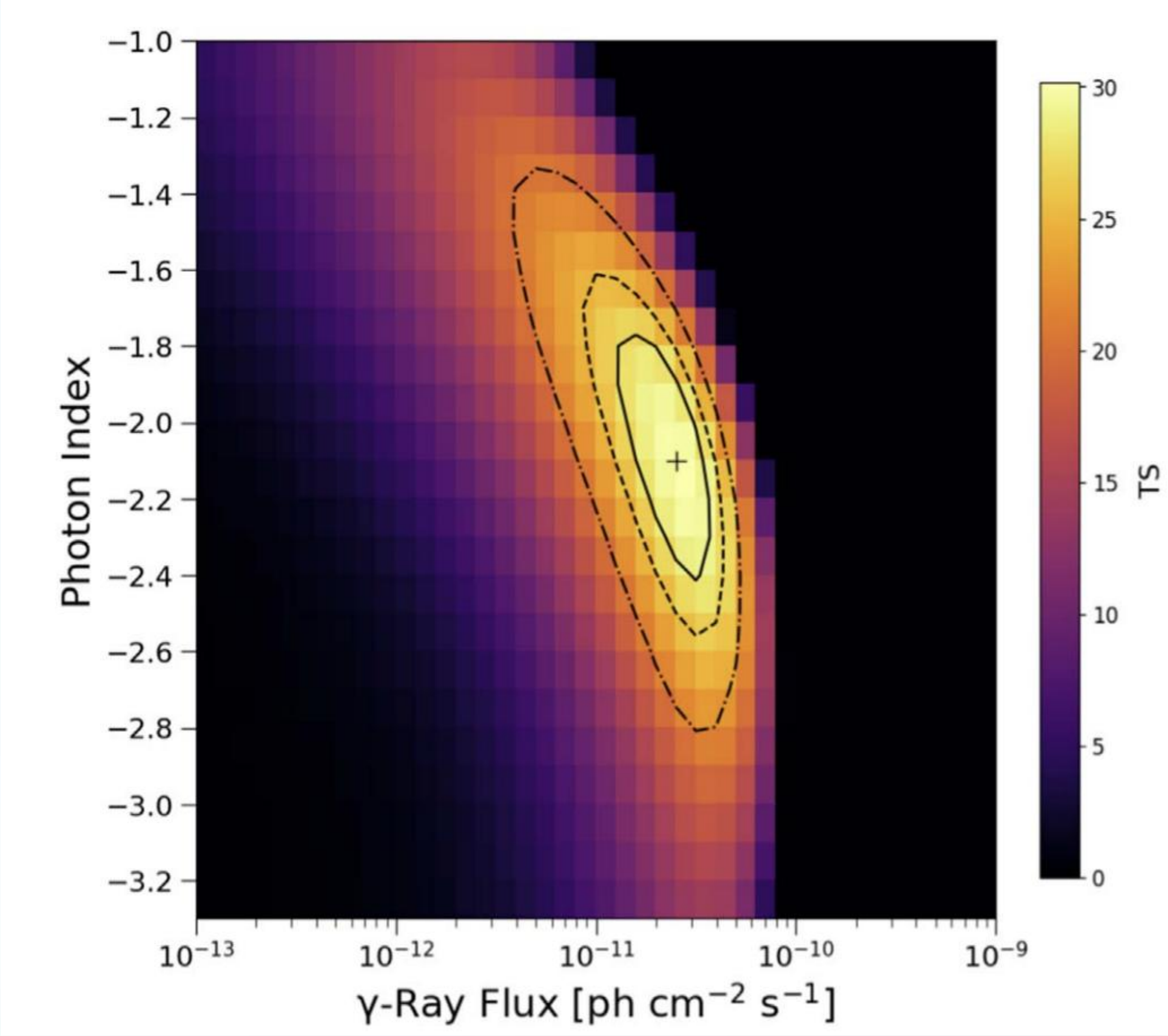


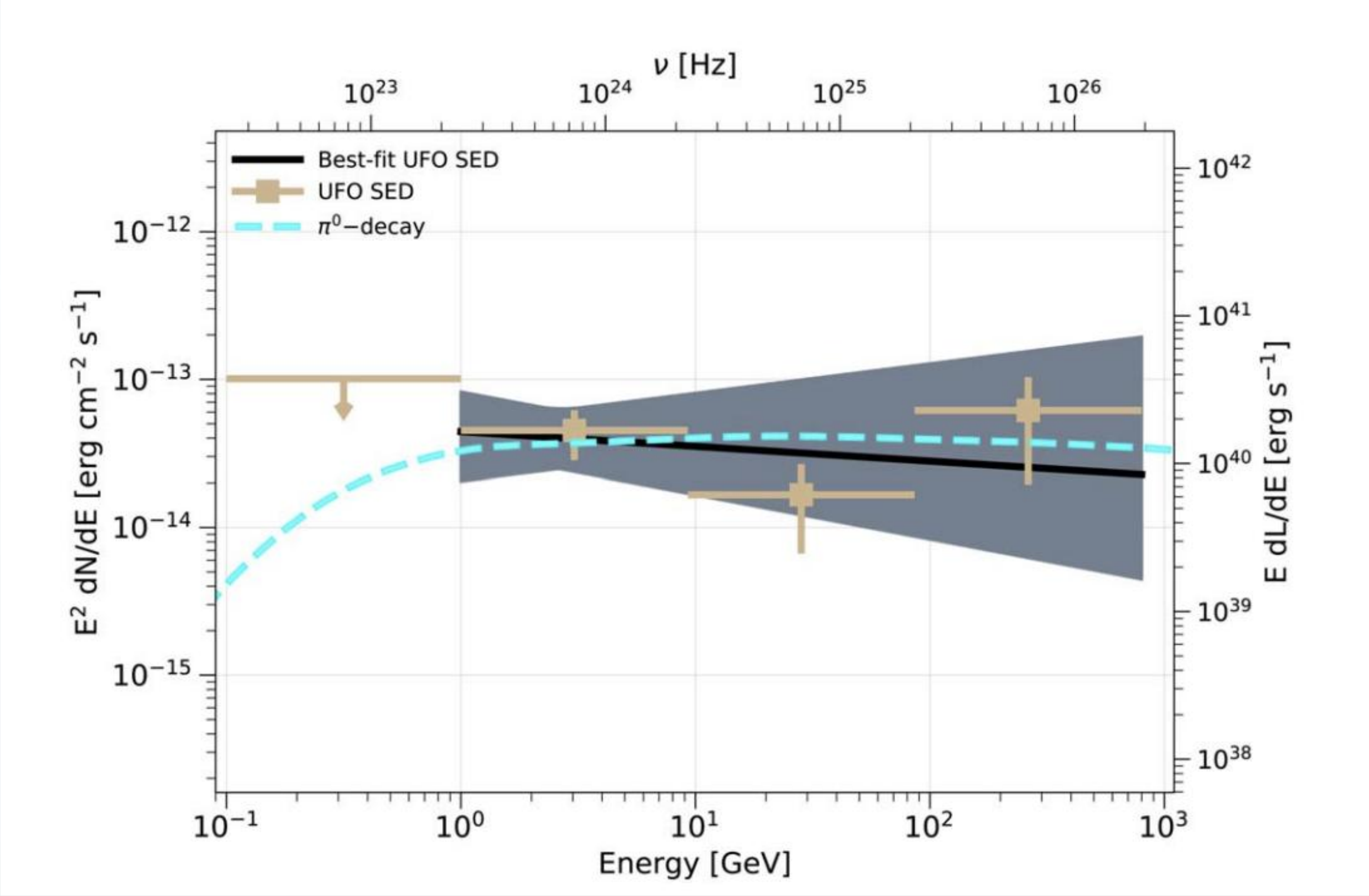


**Table 1**
UFO Source Sample

| Name (1) | R.A. (deg) [J2000] (2) | Decl. (deg) [J2000] (3) | Type (4) | Redshift [z] (5) | Velocity [v/c] (6) | $\log M_{BH}$ [$M_\odot$] (7) | $\log \dot{E}_K^{Min}$ [erg s$^{-1}$] (8) | $\log \dot{E}_K^{Max}$ [erg s$^{-1}$] (9) | $\log L_{Bol}$ [erg s$^{-1}$] (10) | 95% UL ($\times 10^{-11}$) [ph cm$^{-2}$ s$^{-1}$] (11) |
|---|---|---|---|---|---|---|---|---|---|---|
| Ark 120[a,c] | 79.05 | −0.15 | Sy1 | 0.033 | 0.27 | 8.2 ± 0.1 | >43.1 | 46.2 ± 1.3 | 45.0[f]<br>44.2[h]<br>**44.6** | 7.5 |
| MCG-5-23-16[a,c] | 146.92 | −30.95 | Sy2 | 0.0084 | 0.12 | 7.6 ± 1.0 | 42.7 ± 1.0 | 44.3 ± 0.2 | 44.1[l] | 4.3 |
| NGC 4151[a,c] | 182.64 | 39.41 | Sy1 | 0.0033 | 0.105 | 7.1 ± 0.2 | >41.9 | 43.1 ± 0.5 | 44.1[g]<br>42.9[h]<br>43.9[i]<br>42.9[j]<br>43.2[k]<br>**43.4** | 10.6 |
| PG 1211+143[a,c] | 183.57 | 14.05 | Sy1 | 0.081 | 0.13 | 8.2 ± 0.2 | 43.7 ± 0.2 | 46.9 ± 0.1 | 45.7[f]<br>44.8[h]<br>44.7[j]<br>45.0[k]<br>**45.1** | 3.7 |
| NGC 4507[a,c] | 188.90 | −39.91 | Sy2 | 0.012 | 0.18 | 6.4 ± 0.5 | >41.2 | 44.6 ± 1.1 | 44.3[e] | 3.4 |
| NGC 5506[b,d] | 213.31 | −3.21 | Sy1.9 | 0.006 | 0.25 | 7.3 ± 0.7 | 43.3 ± 0.1 | 44.7 ± 0.5 | 44.3[e] | 6.4 |
| Mrk 290[a,c] | 233.97 | 57.90 | Sy1 | 0.030 | 0.14 | 7.7 ± 0.5 | 43.4 ± 0.9 | 45.3 ± 1.2 | 44.4[e] | 4.5 |
| Mrk 509[a,c] | 311.04 | −10.72 | Sy1 | 0.034 | 0.17 | 8.1 ± 0.1 | >43.2 | 45.2 ± 1.0 | 45.2[e]<br>44.3[h]<br>45.3[i]<br>44.3[j]<br>44.5[k]<br>**44.7** | 9.5 |
| SWIFT J2127.4 +5654[b,d] | 321.94 | 56.94 | Sy1 | 0.014 | 0.23 | ∼7.2 | 42.8 ± 0.1 | 45.6 ± 0.5 | 44.5[d] | 9.1 |
| MR 2251-178[b,d] | 343.52 | −17.58 | Sy1 | 0.064 | 0.14 | 8.7 ± 0.1 | 43.3 ± 0.1 | 46.7 ± 0.7 | 45.8[f] | 7.4 |
| NGC 7582[a,c] | 349.60 | −42.37 | Sy2 | 0.0052 | 0.26 | 7.1 ± 1.0 | 43.4 ± 1.1 | 44.9 ± 0.4 | 43.3[e] | 4.7 |

# Summary:

1. SS 433 is a powerful & bright microquasar shining in gamma-ray band, from GeV to above 100 TeV.

2. Particle acceleration from jet and possible relativistic outflows.

3. Energy-dependent TeV morphology and periodic GeV emission of SS 433 support its nature as a hadronic particle accelerator.

# SS 433: Iron line doppler shifted: relativistic hadrons in the jet

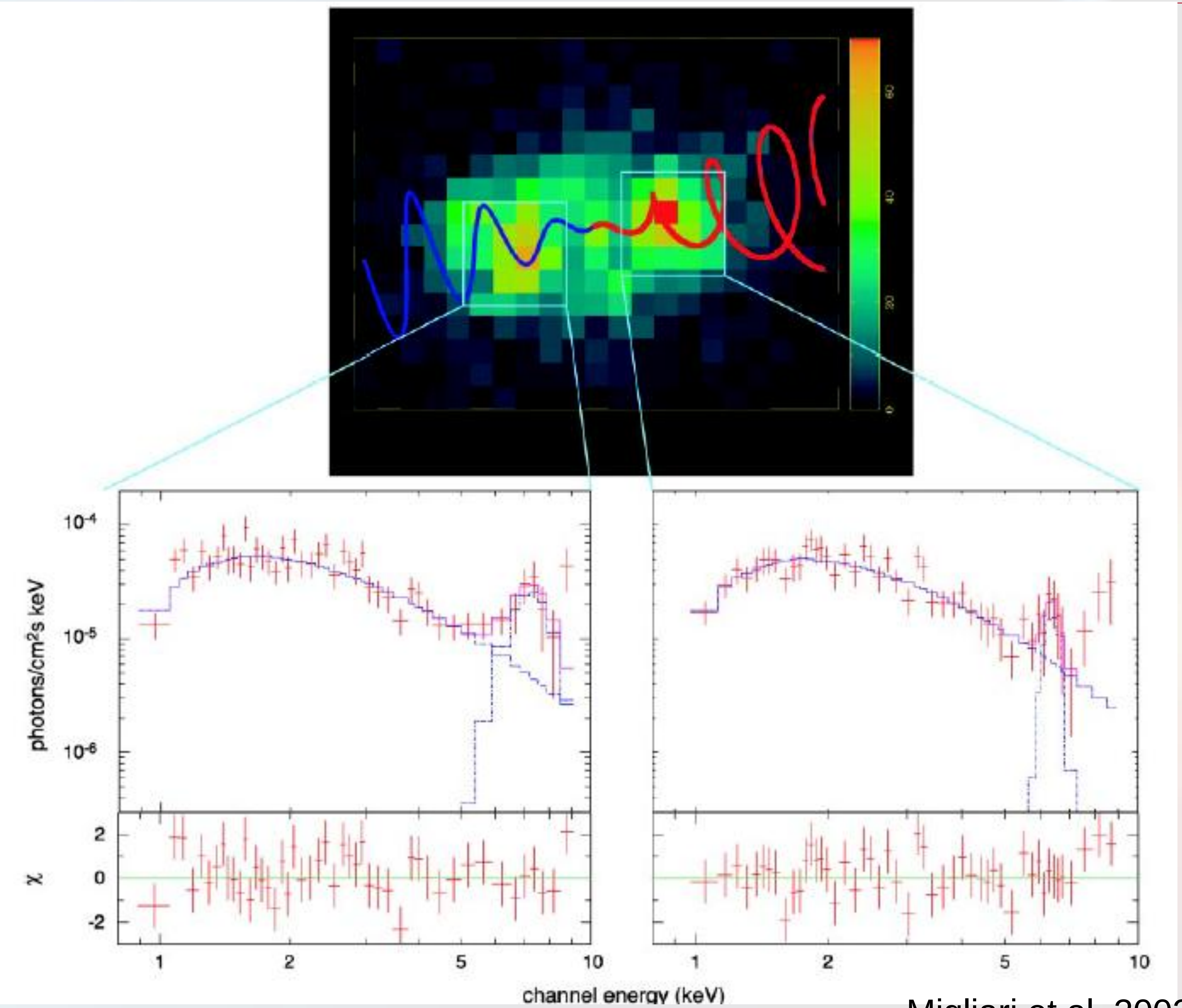


Migliari et al. 2002

# SS 433 in GeV: cloud heart-beating via anisotropic diffusion?

Chandra image in 0.3-10 keV (Li et al. 2025, in prep)

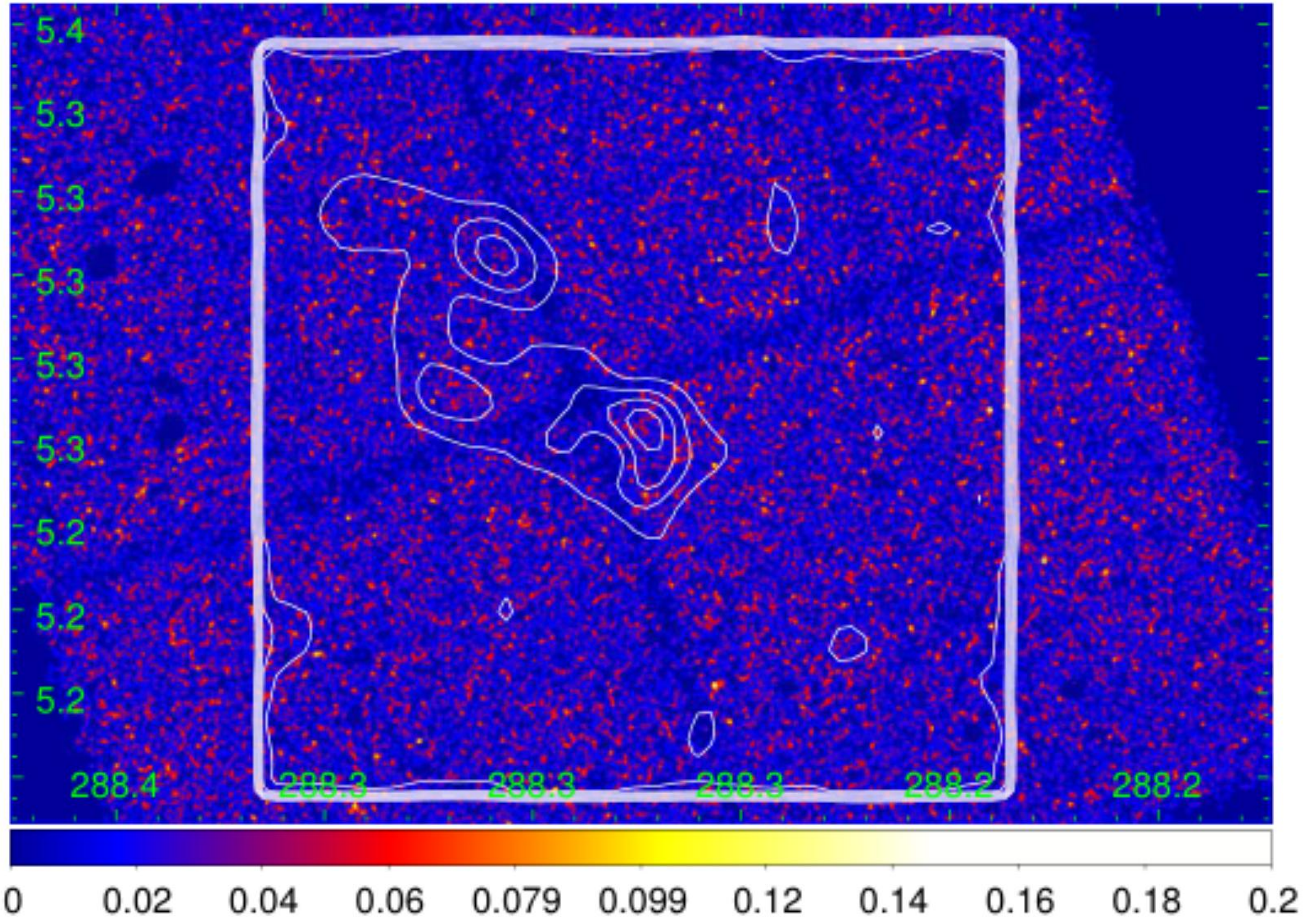


Point sources removed


Jet termination shock
Persistent or transient jet
Shock driven by disk wind
Corona
Central BH (Penrose process; centrifugal force at BH magnetosphere)
Relativistic outflow
Probe of high-energy particle acceleration
X-ray
Gamma-ray
synchrotron (electrons)
IC / $\pi^0$ decay (electrons/protons)
contamination
Thermal X-ray emission from hot gas and accretion disk